



TID nowcasting models – LSTIDs

Antoni Segarra
Ebro Observatory
asegarra@obsebre.es



Training School PITHIA-NRF / T-FORS
5-9 February 2024. Leuven (Belgium)



Outline

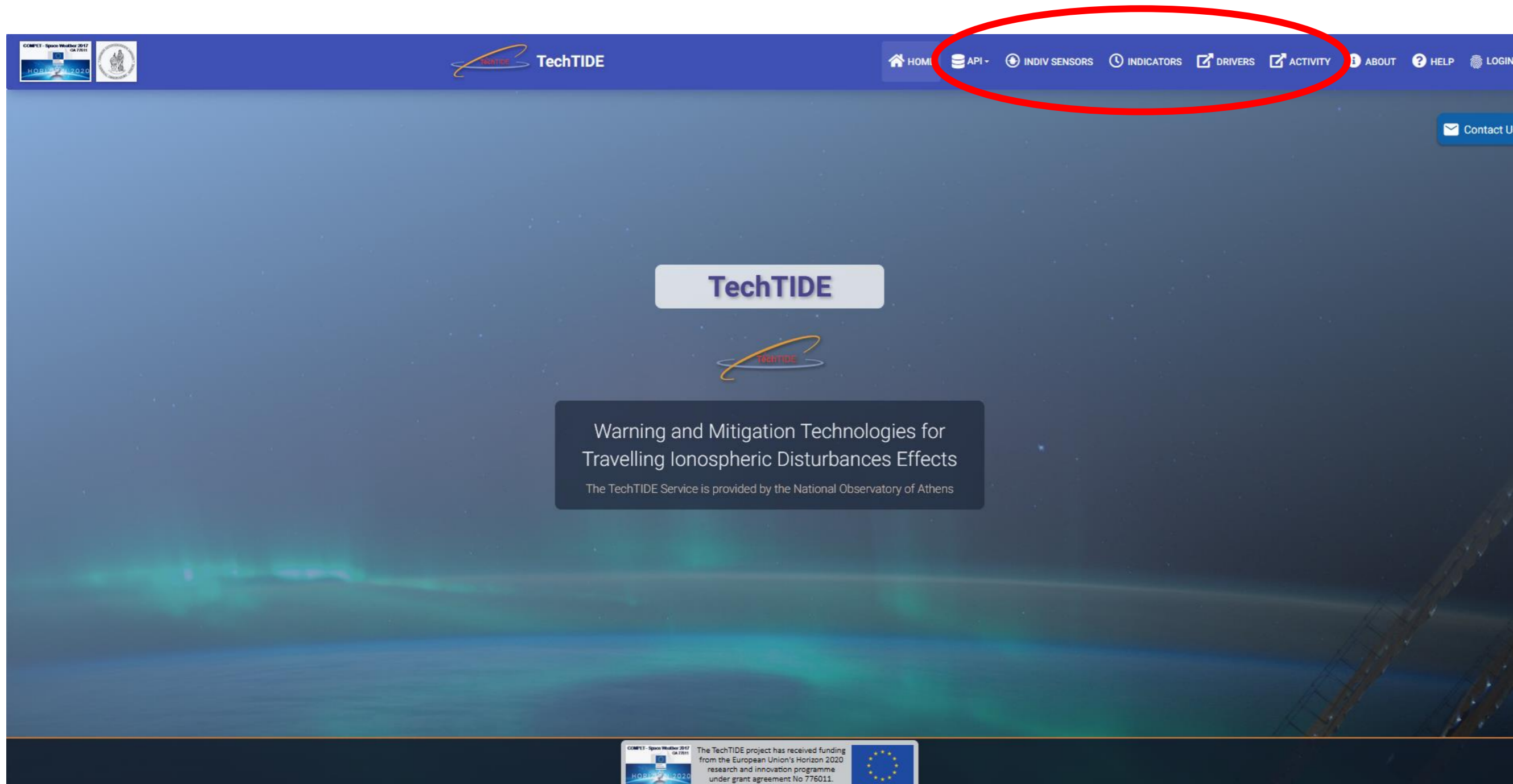
- TechTIDE products:
 - HF-Interferometry (HF-Int)
 - HTI
 - HF TID map (D2D)
 - Indicators
- GNSS
 - Case studies



TechTIDE Products



[TechTIDE Portal](#) also available through the PITHIA-NRF [e-Science Center](#) at [TechTIDE LSTID activity index](#) Data Collection.



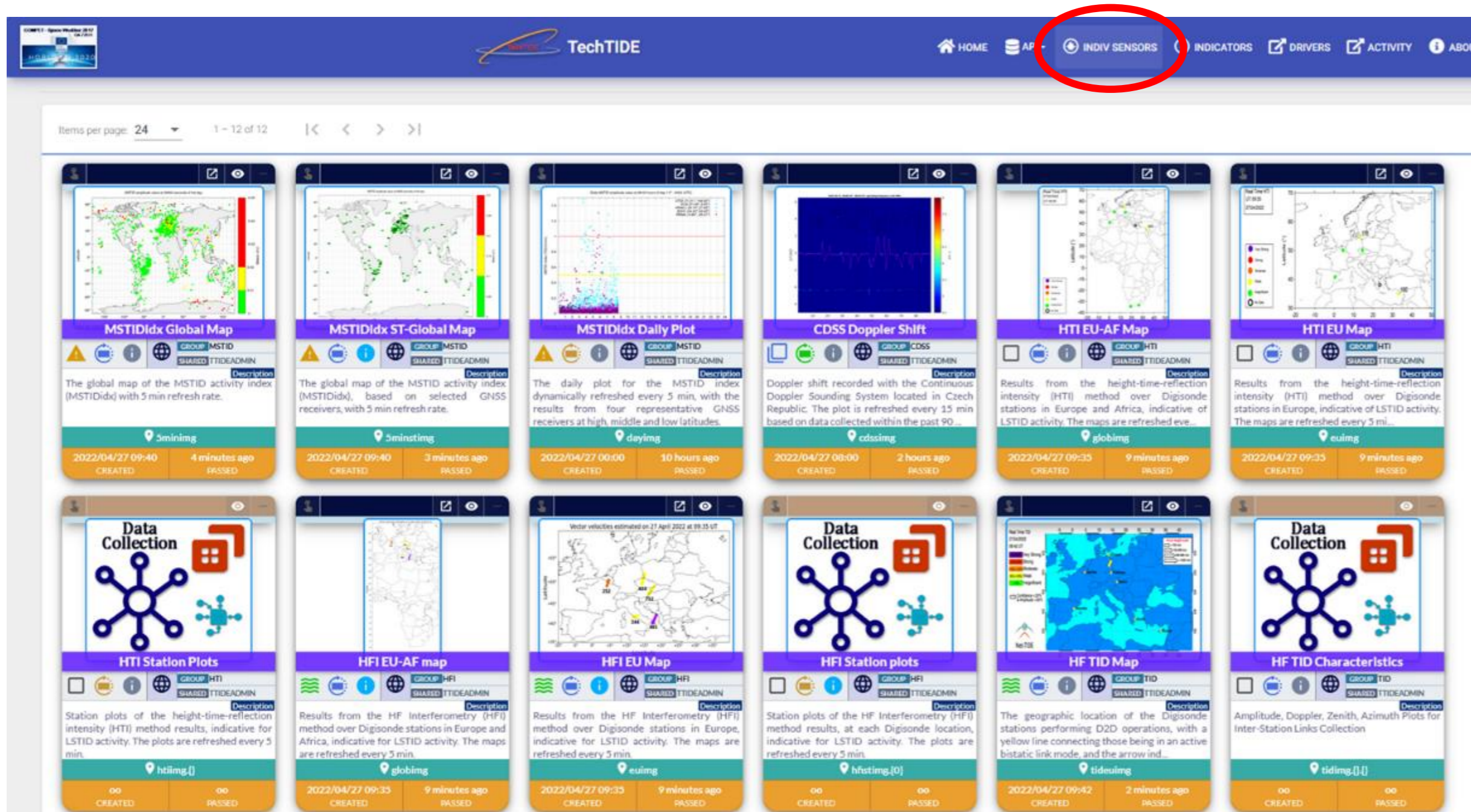
- API
- Sensors
- Indicators
- Drivers
- Activity



TechTIDE Products



[TechTIDE Portal](#) also available through the PITHIA-NRF [e-Science Center](#) at [TechTIDE LSTID activity index](#) Data Collection.



- HTI (High-time-reflection intensity)
- HFI (HF Interferometry)
- HF TID (D2D)



TechTIDE Products



Log in only in current section

Search Site Search

Home TechTIDE Warning Services Community TID Detection Dissemination & Communication

News Wiki

Home TID Detection Repository

Methodologies
Repository
Impact

Repository

ID	Code Name	User Manual	Code File	Terms and Conditions
1	Electron Density Distribution	Download User Manual	Download Code File	<p>This is an Open Access code, distributed under the terms of the Creative Commons Attribution License, which permits unrestricted use, distribution, and reproduction in any medium, provided the original work is cited as follows:</p> <ul style="list-style-type: none"> Belehaki, A., I. Tsagouri, I. Kutiev, P. Marinov, and S. Fidanova. Upgrades to the Topside Sounders Model assisted by Digisonde (TaD) and its validation at the topside ionosphere. J. Space Weather Space Clim., 2, A20, 2012, DOI: http://dx.doi.org/10.1051/swsc/2012020. Kutiev I., P. Marinov, S. Fidanova, A. Belehaki and I. Tsagouri, Adjustments of the TaD electron density reconstruction model with GNSS-TEC parameters for operational application purposes, J. Space Weather Space Clim. 2 A21 (2012), DOI: http://dx.doi.org/10.1051/swsc/2012021.

Codes of the TechTIDE methods available at [repository](#)

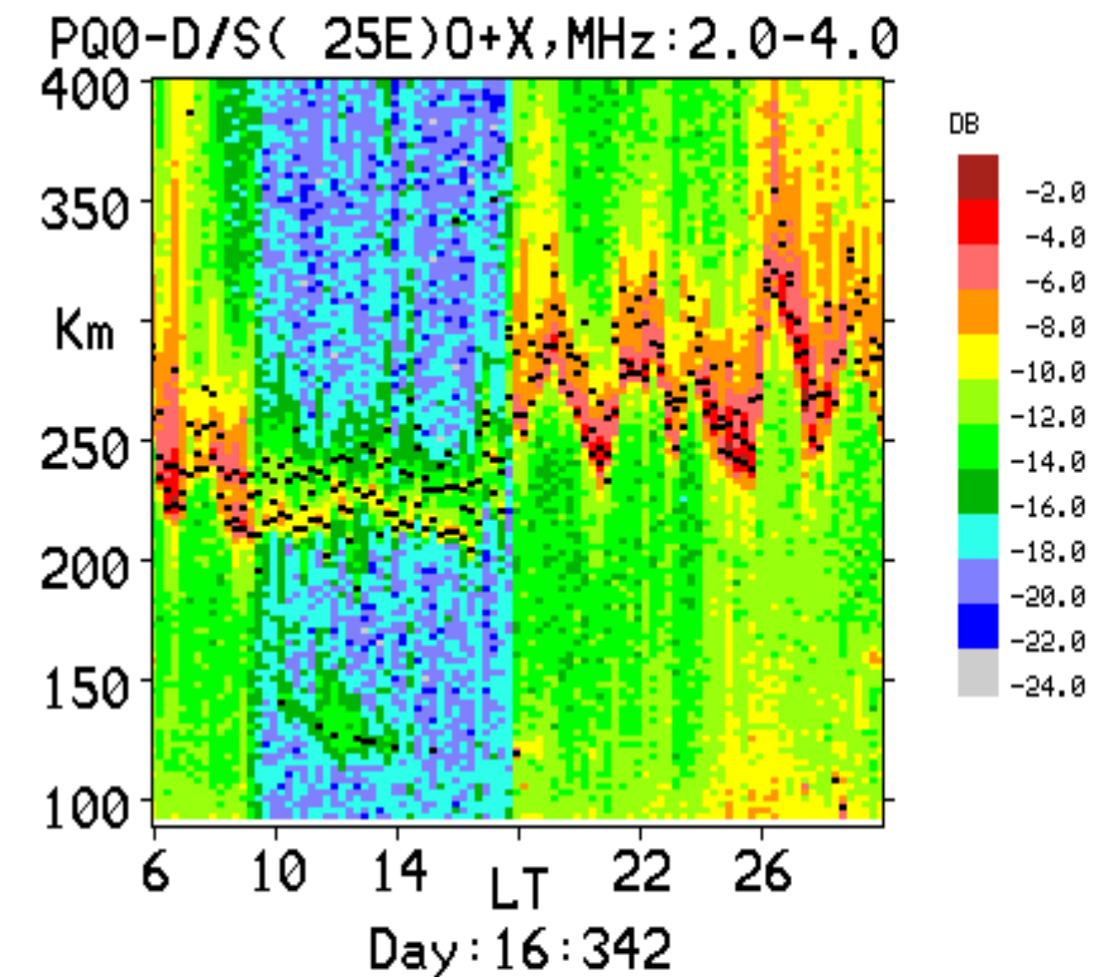
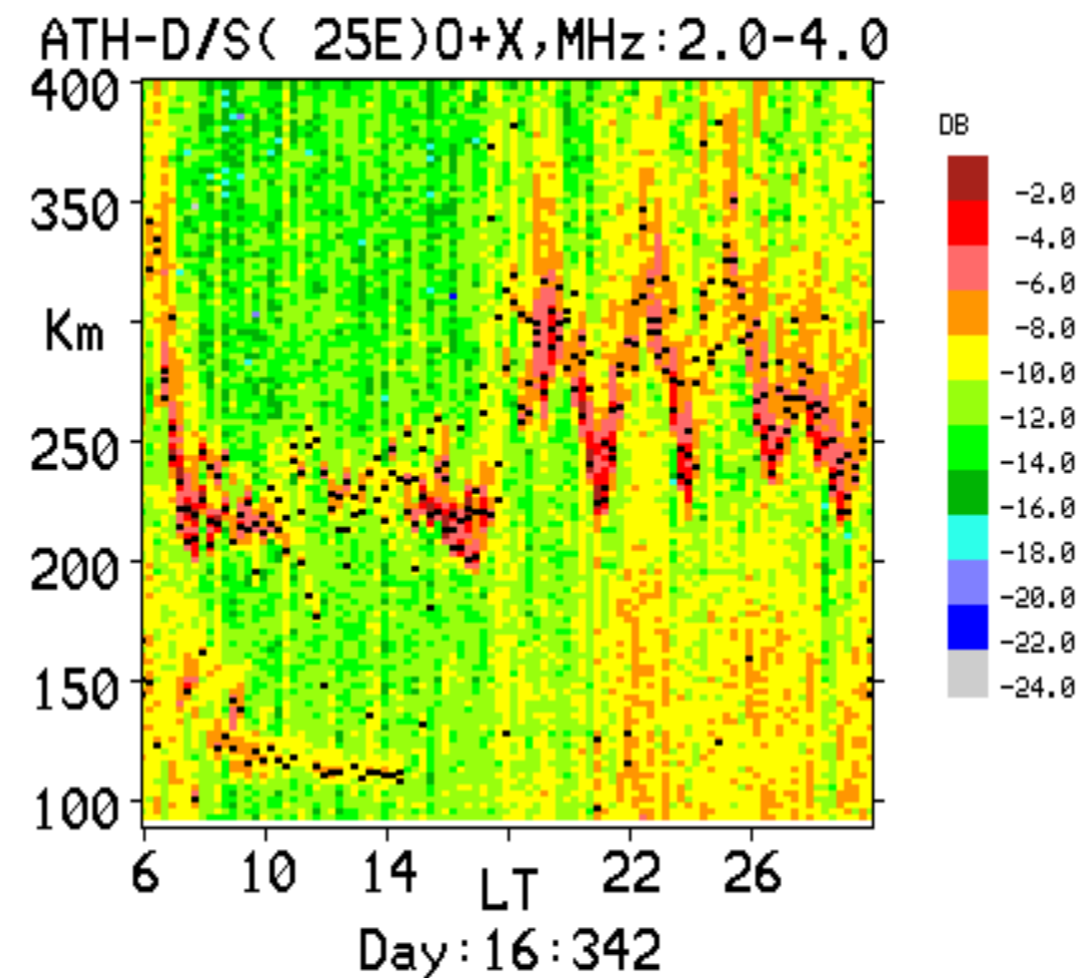
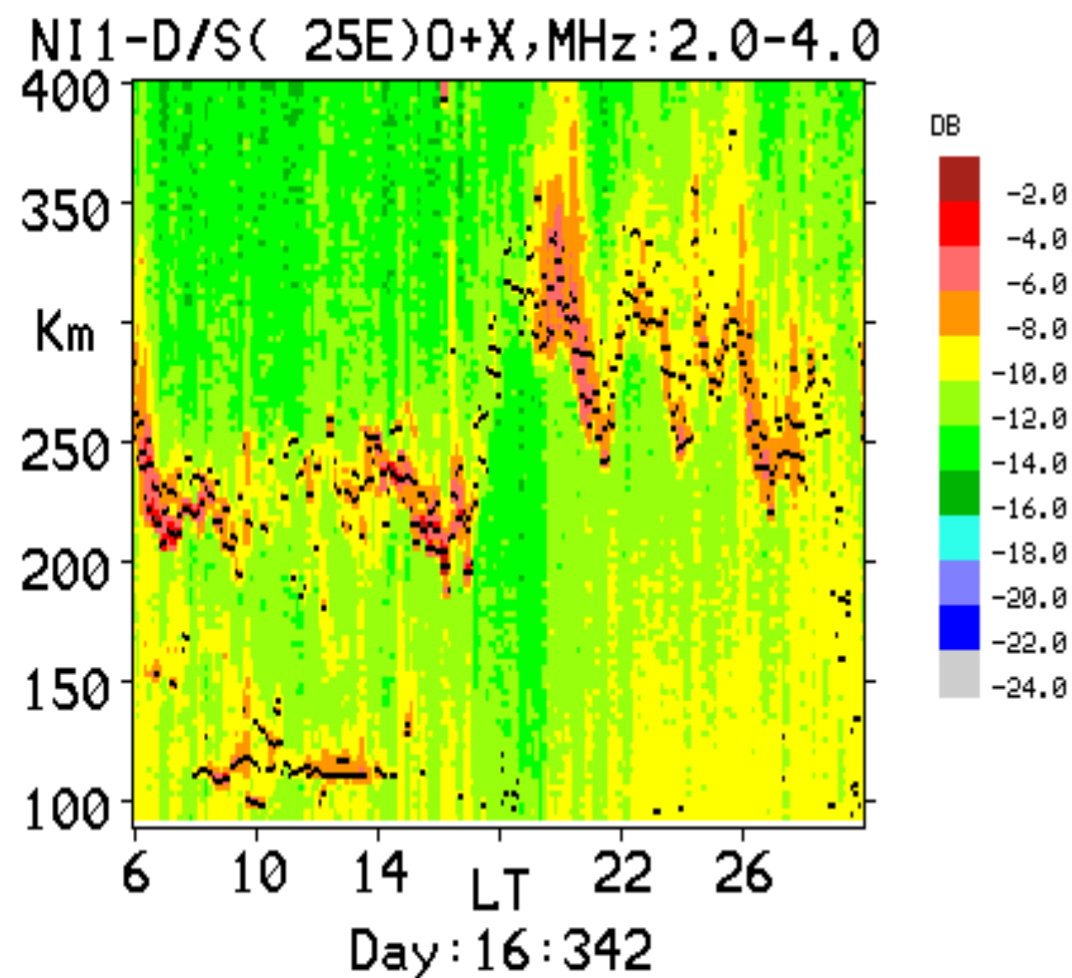


HTI Hight-Time-reflection Intensity method

IdN. Method	Main Characteristics	Intermediate Product	Final Product	Value added Product
HTI Reconstructs daily plot of the vertical movement of the ionospheric layers and it can capture oscillations detected in space from all possible sources.	Input: raw vertical ionogram binary data from single station Output: Reconstructed daily variability of F region virtual height.	F region virtual height variation above a given Digisonde station	Period of dominant wave activity.	Relative contribution of detected LSTID to the total variance

HTI High-Time-reflection Intensity method

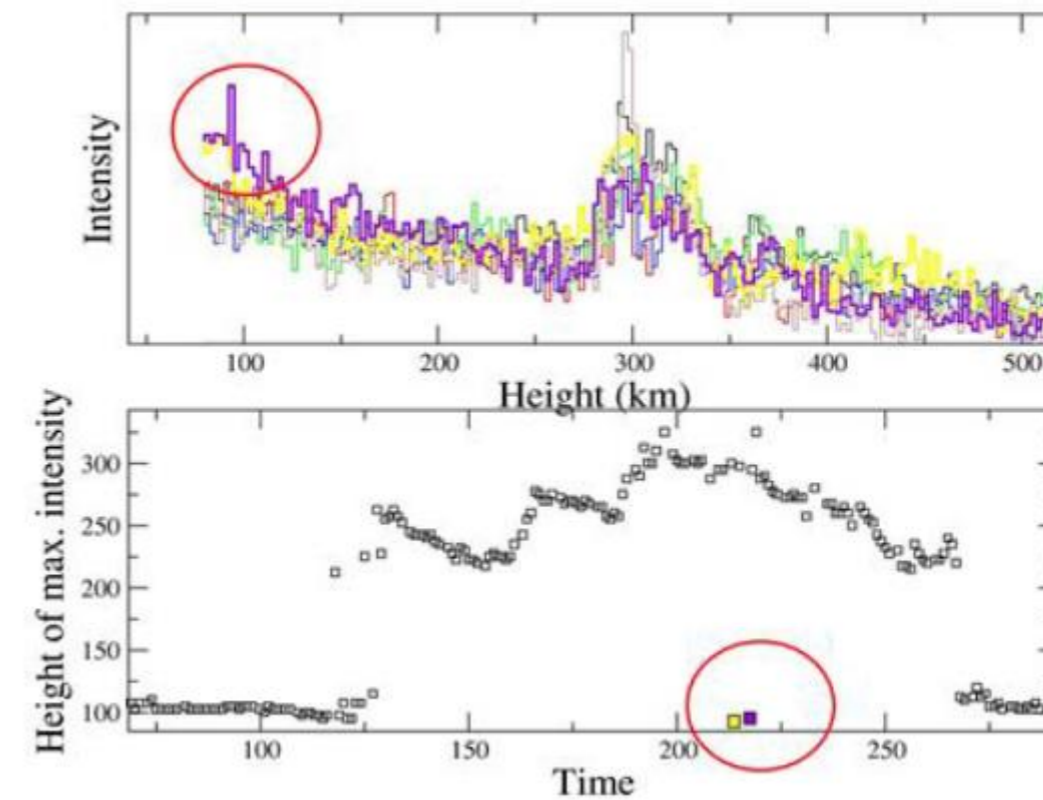
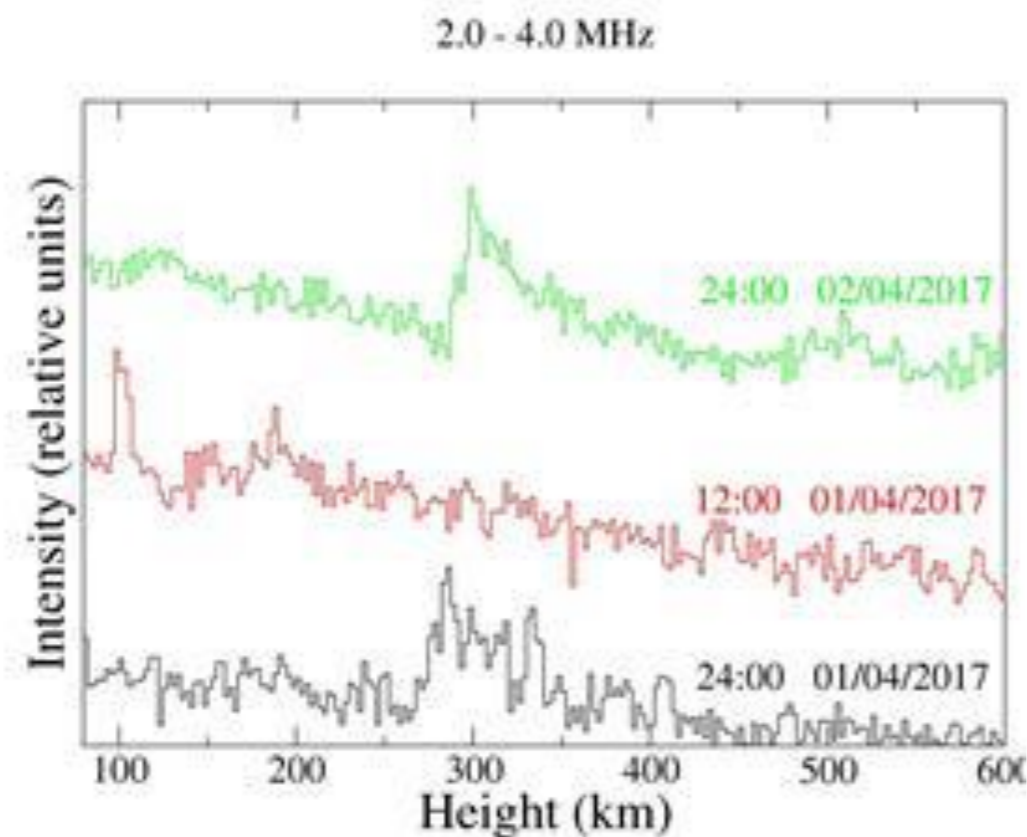
HTI uses the actual ionograms produced over each station. HTI considers an ionogram as a “snapshot” of reflected intensity as a function of height and Digisonde signal frequency, and it uses a sequence of ionograms to compute an average HTI plot, (for a given frequency bin) reflected signal-to-noise ratio in dB [Haldoupis et al. 2006].



HTI High-Time-reflection Intensity method

HTI also uses near real time foF2 data from the [GIRO](#) to estimate the optimal frequency bin within which the F-region trace of the ionograms will be processed at each instant during a 24-hour interval.

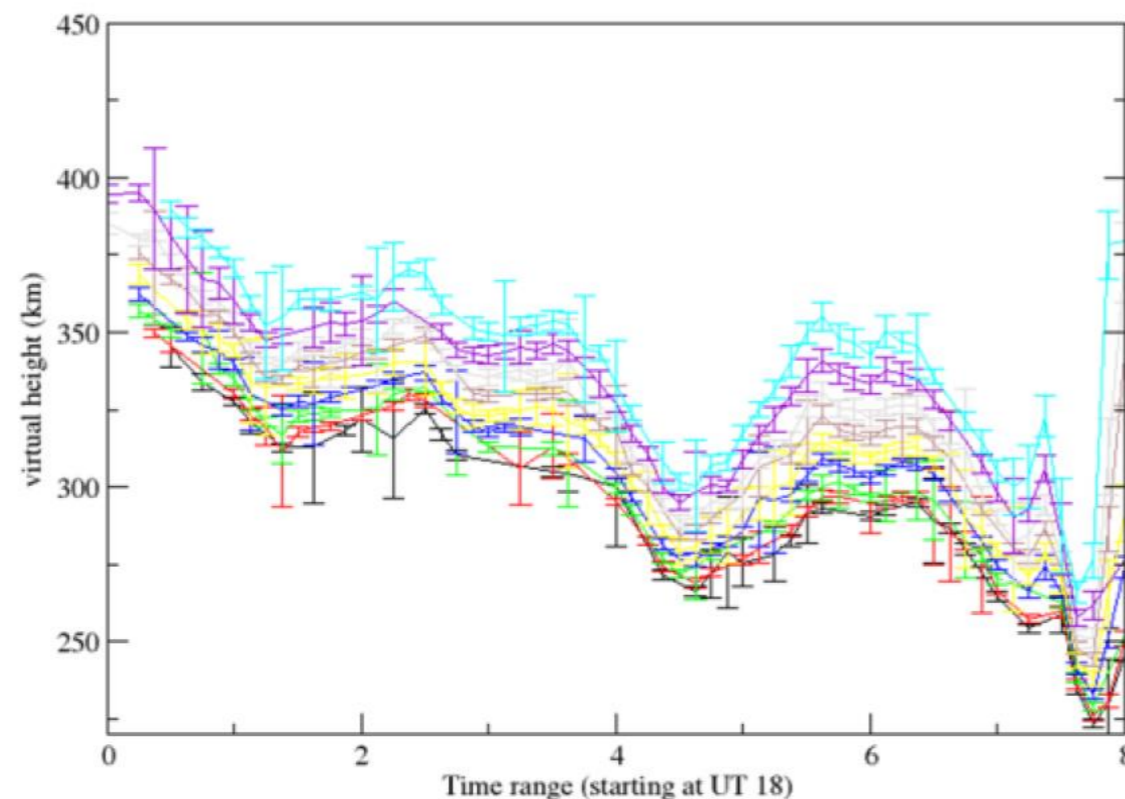
Superimposing virtual height profiles, the points of maximum intensity can be obtained. Strong reflections from sporadic E (Es) could be strong enough to mask F-region reflections so appropriate procedures have been applied to treat these points as outliers.



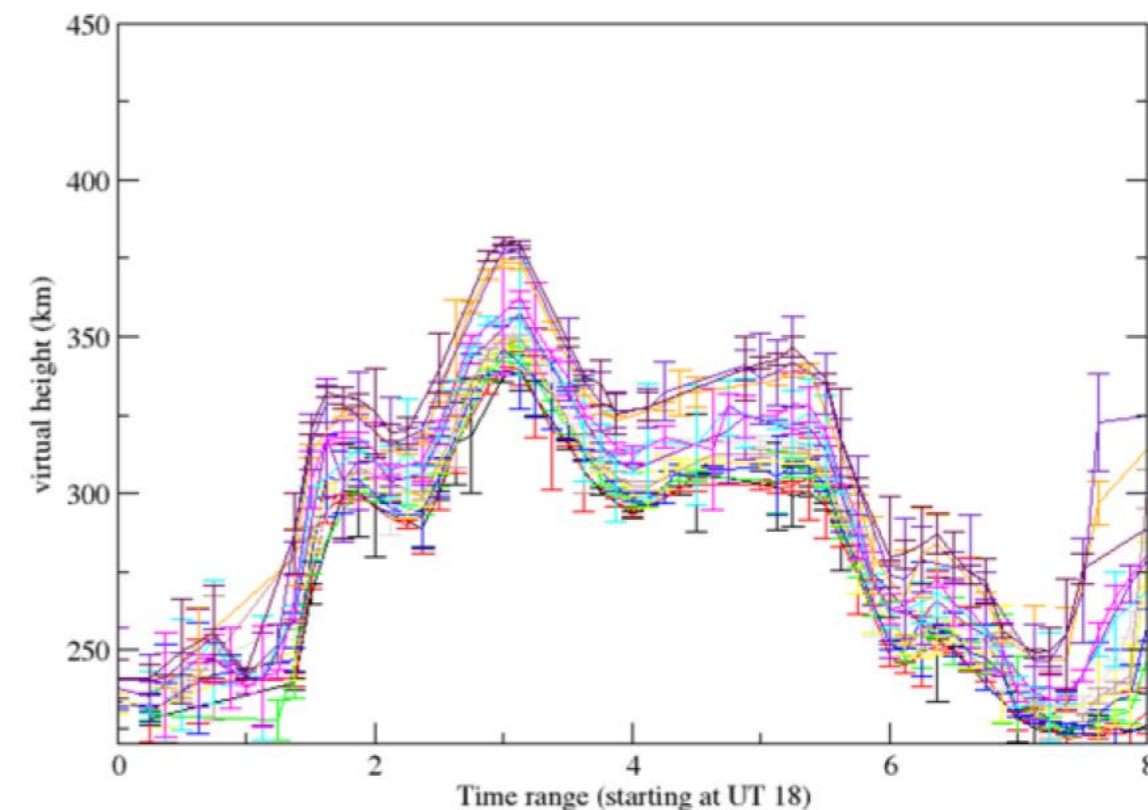
HTI High-Time-reflection Intensity method

HTI exploits multiple narrow frequency bins to overcome interference causing gaps on ionogram traces. For each frequency bin at each time interval, obtaining a value of the virtual height with an appropriate uncertainty (as the standard deviation). To enhance the reliability of the method, the X-mode trace is taken into the measurements. This is particularly significant when the O-mode ionogram trace is not well defined.

HTI for NI135. Year=17 Day=81 UT=18:00



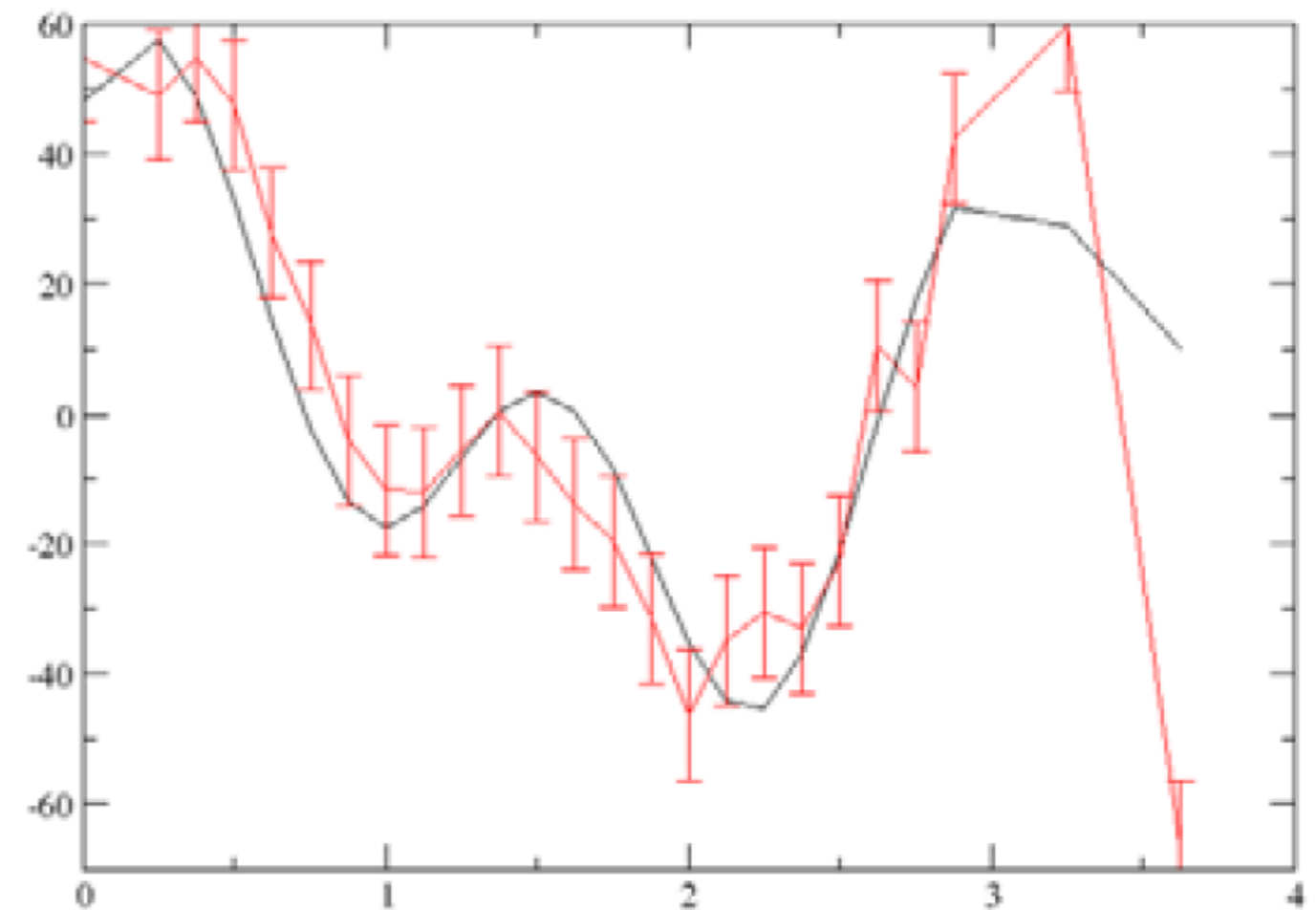
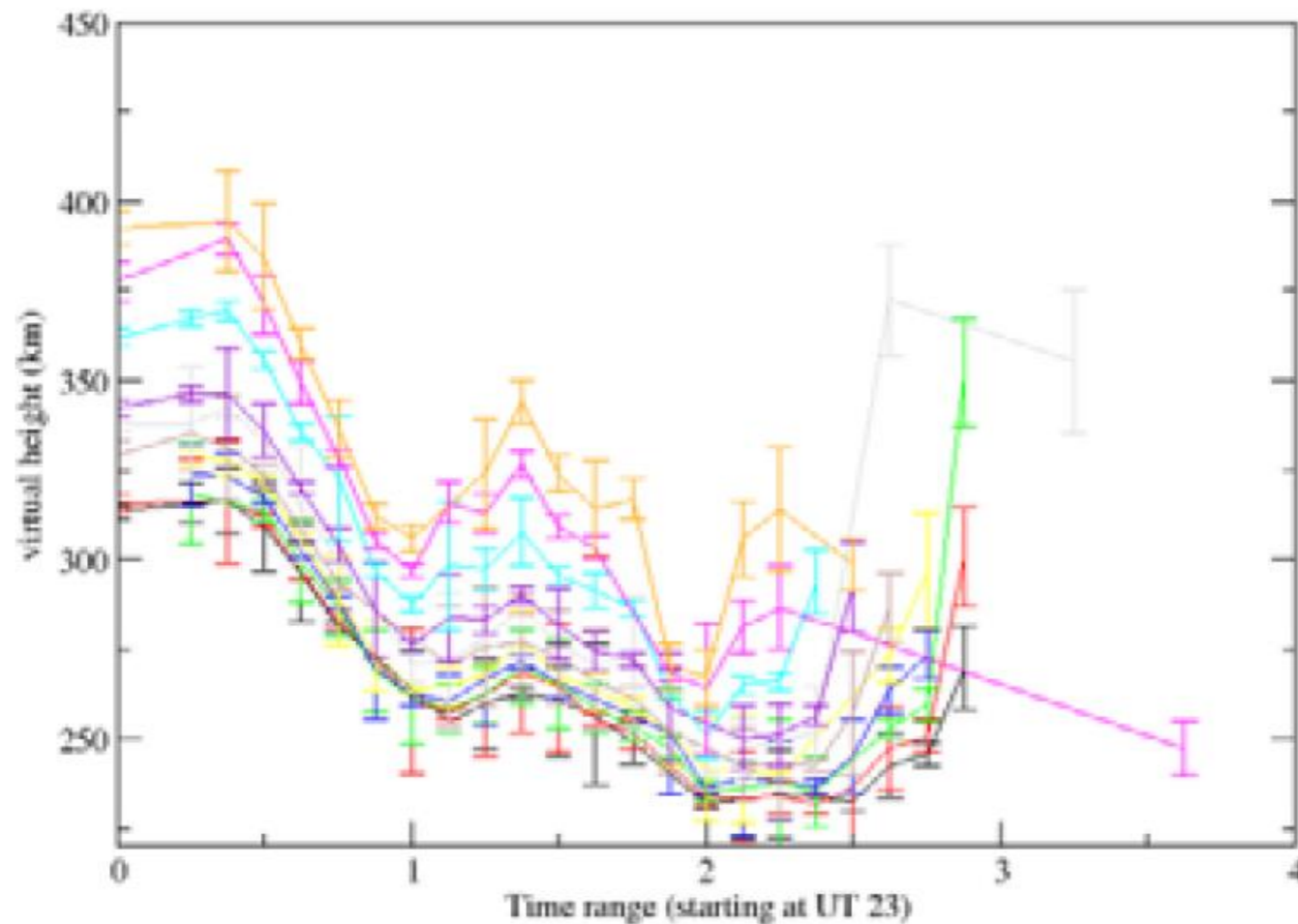
HTI for NI135. Year=17 Day=111 UT=18:00



HTI High-Time-reflection Intensity method

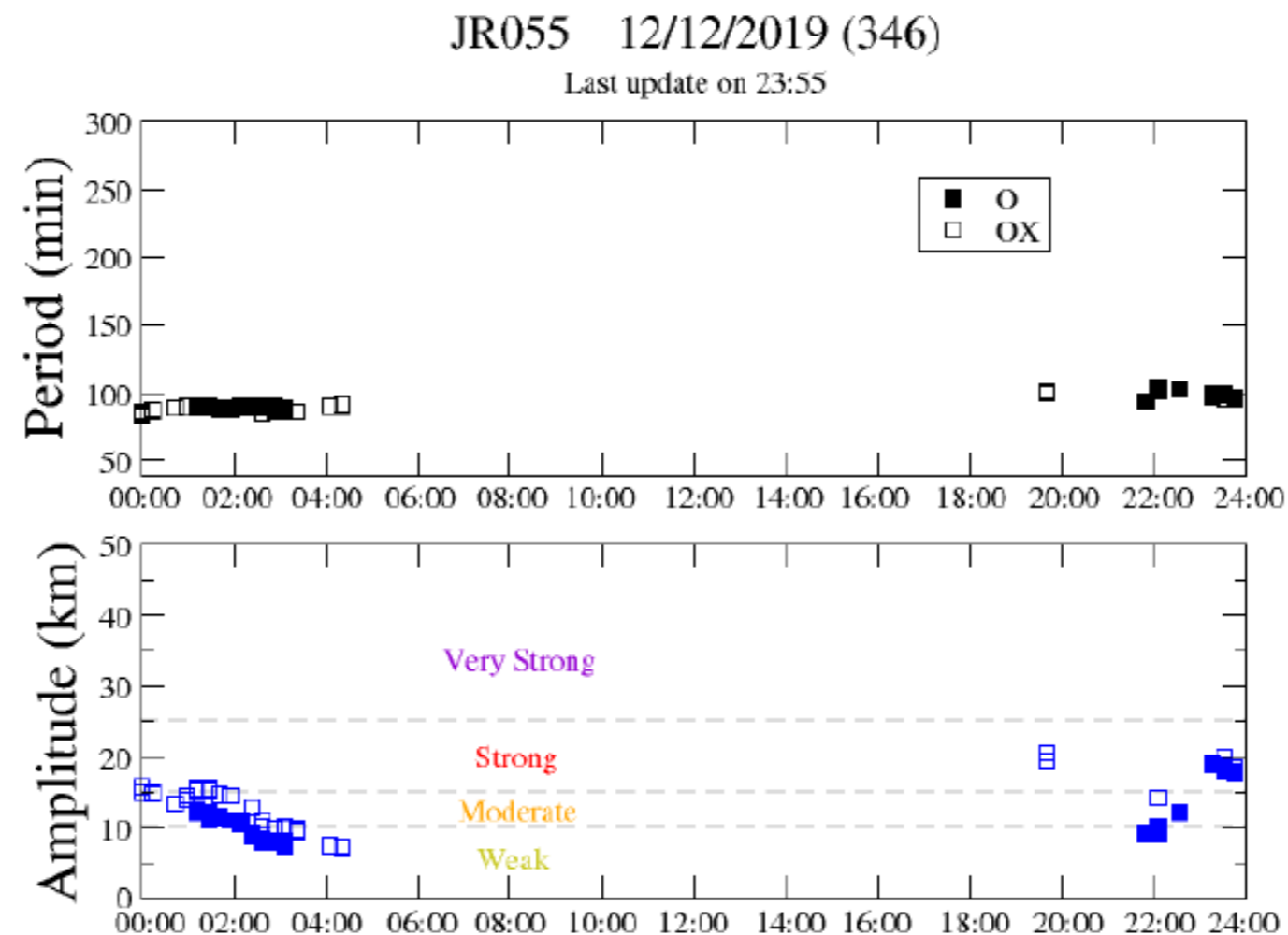
The virtual height variation on various frequency bins is then reduced to a representative signal by removing from each the average background and a statistical fitting technique is then applied to examine how well a sinusoidal model describes the data.

HTI for NI135. Year=17 Day=111 UT=23:00



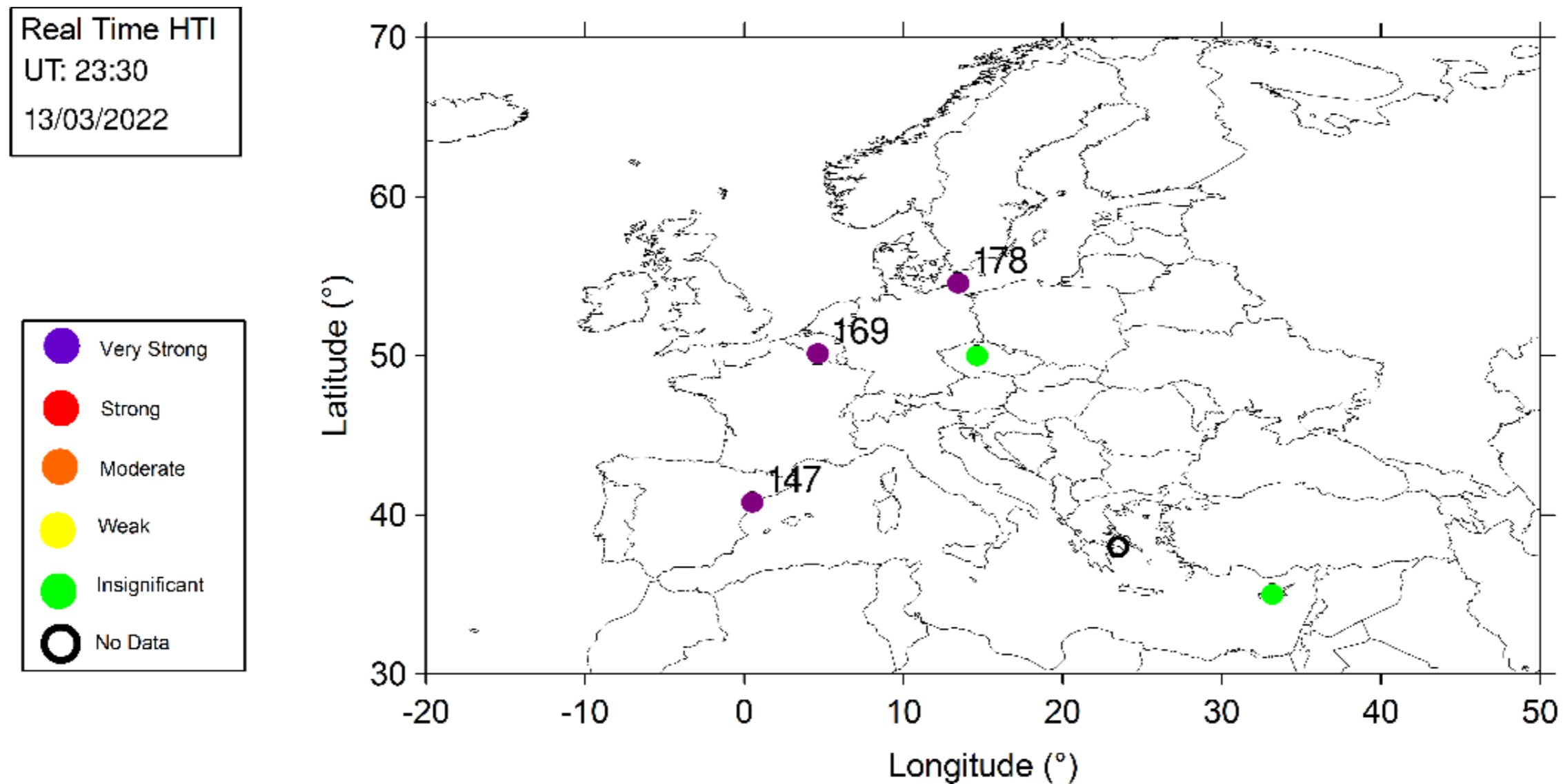
HTI High-Time-reflection Intensity method: Products

The final product of the HTI over a station outputs the analysis results from independently processing O (black rectangles) and O and X traces (white rectangles). Identifying coincidence of the two independent results which underlines the validity of the calculated periodicity.



HTI High-Time-reflection Intensity method: Products

A Europe map with the activity level and the value of the periodicity is given every 5 minutes.

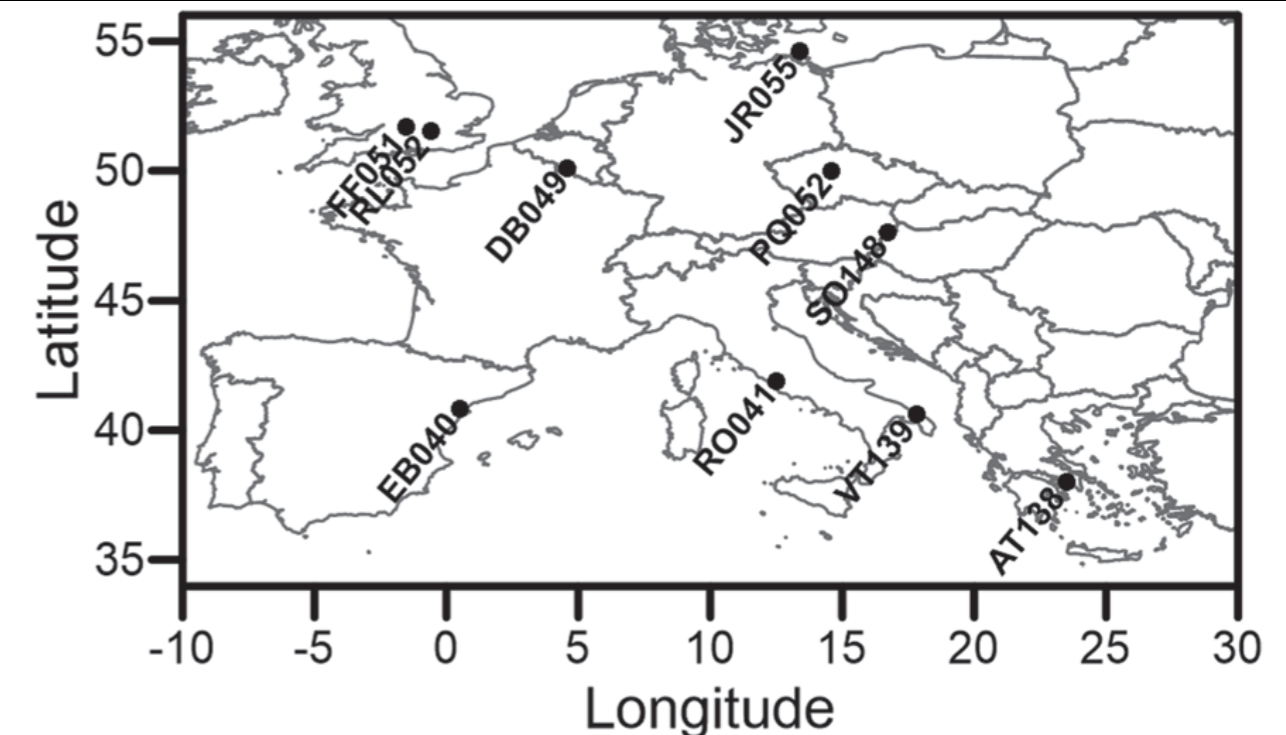
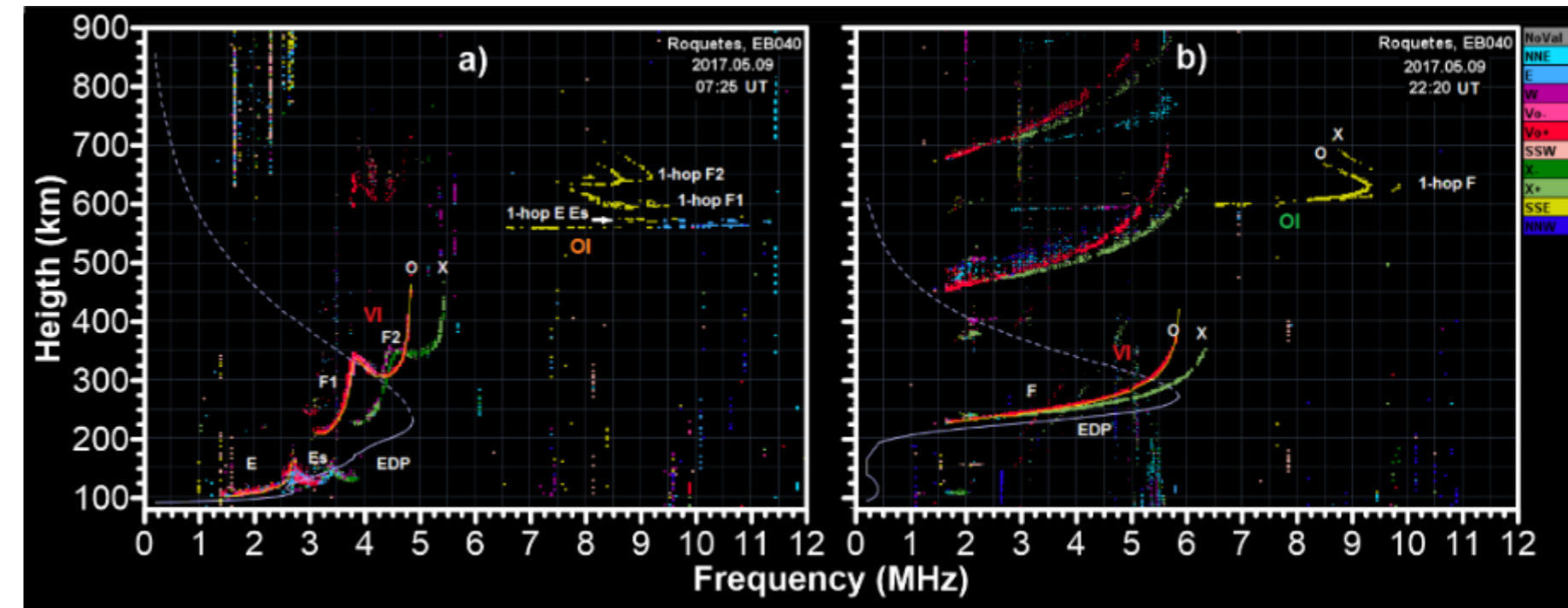


HF-Interferometry (HFI) method

IdN. Method	Main Characteristics	Intermediate Product	Final Product	Value added Product
HF-INT Finds oscillation activity in ionospheric characteristics and it can detect LSTIDs only.	<u>Input</u> : ionospheric characteristics from VI and OI soundings. <u>Output</u> : 2D TID vector velocity, amplitude and period.	De-trended ionospheric characteristics and contribution of LSTID to the data variability.	Dominant period, Amplitude and 2D Vector velocity of detected LSTID.	Estimation of LSTID propagation

HF-Interferometry (HFI) method

- Characteristics from VI Ionospheric sounding (**MUF(3000)F2**).
- Network of DPS4D with stations working **synchronized**.
- Two versions, one working in **near real time** and another working retrospectively
- Data is obtained from the Global Ionospheric Radio Observatory (GIRO) DIDBase Fast Chars database
<http://giro.uml.edu/didbase/scaled.php>

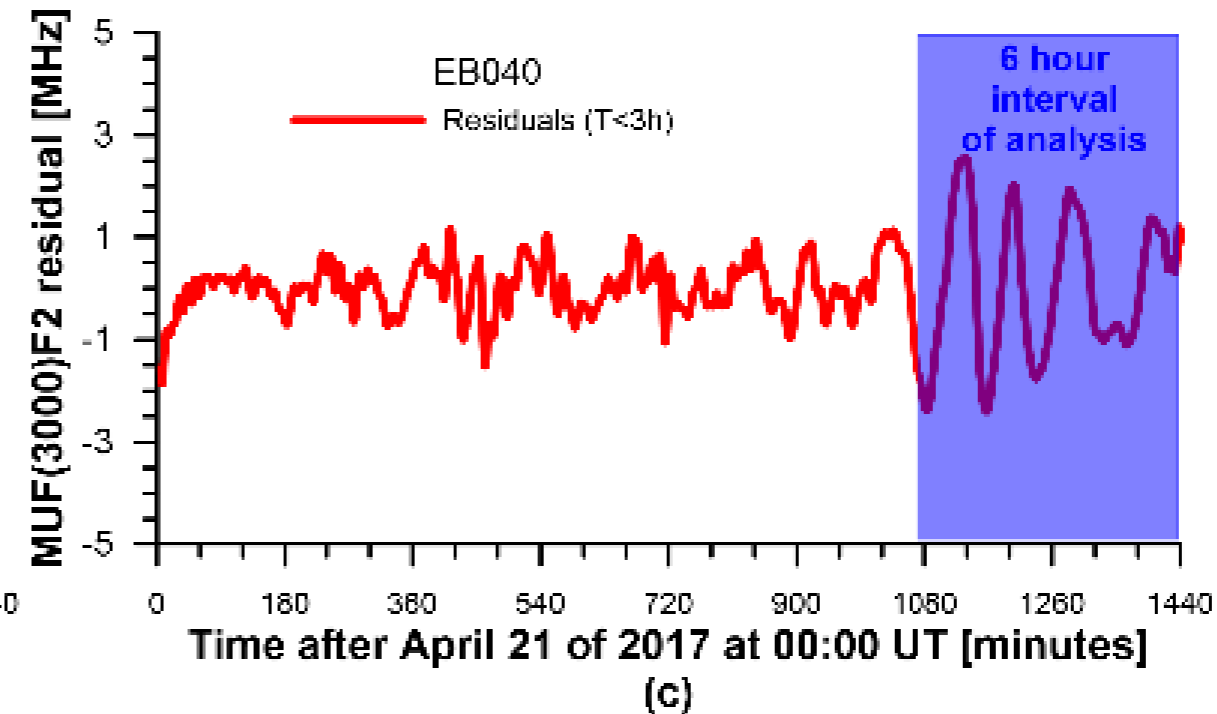
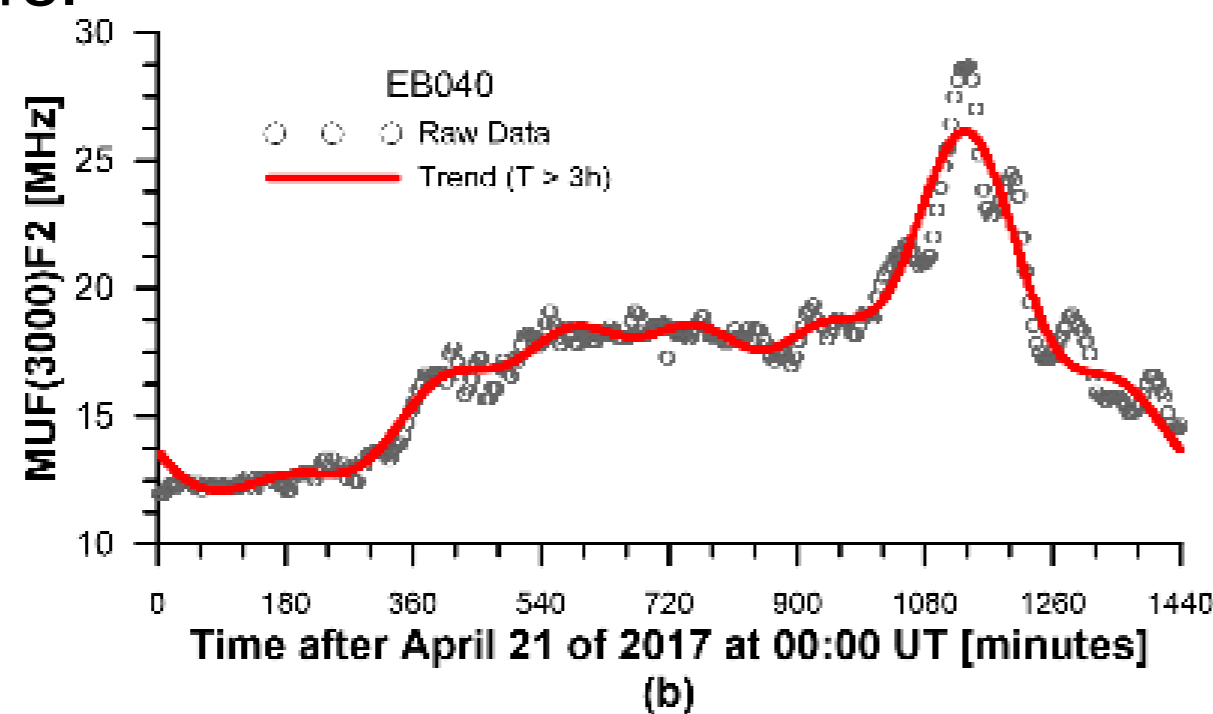


[Altadill et al. 2020]

HF-Interferometry (HFI) method

1.- Data pre-processing

- Discrete Fourier Transform (DFT) interpolation. The original data sampling rate (5–15 min) is rather coarse. With DFT the data is interpolated to increase the sampling rate (upsampling).
- High-pass filtering. The DFT spectrum is high-pass filtered in order to eliminate the slowly varying daily trend. The remaining spectrum produces high frequency residuals which are associated with the wavelike ionospheric disturbances. The data cutoff frequency is the period of 3 hours.



HF-Interferometry (HFI) method

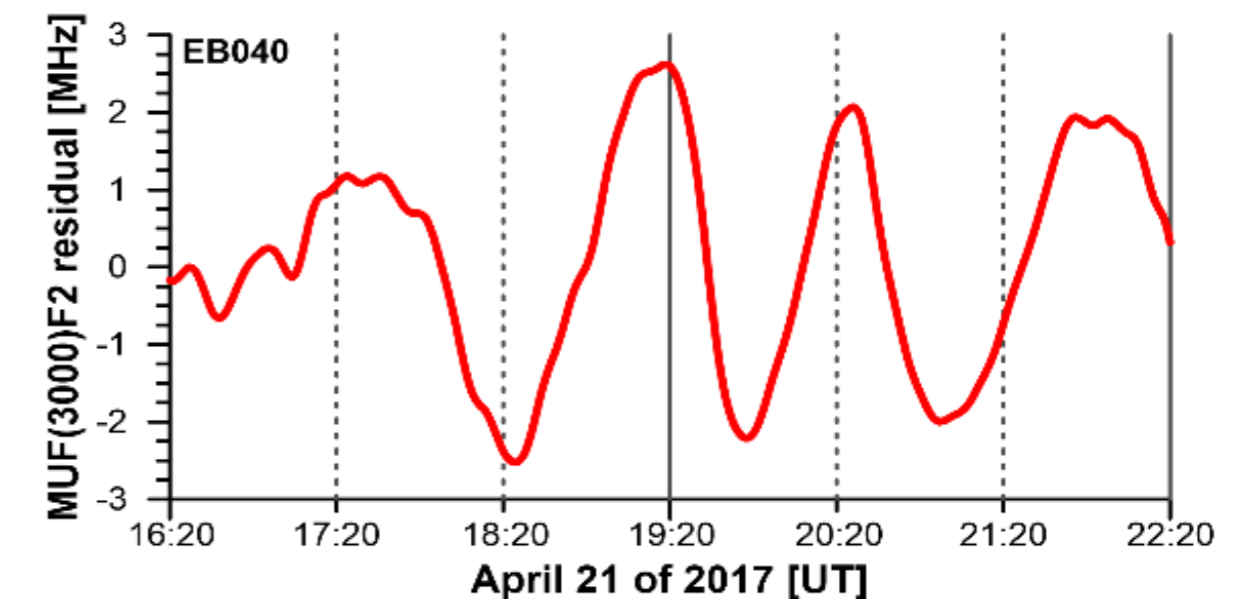
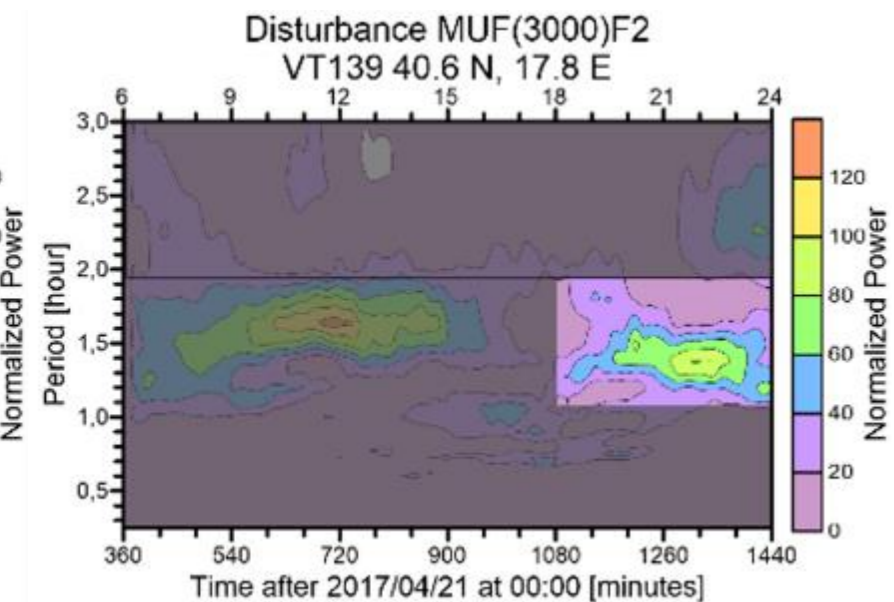
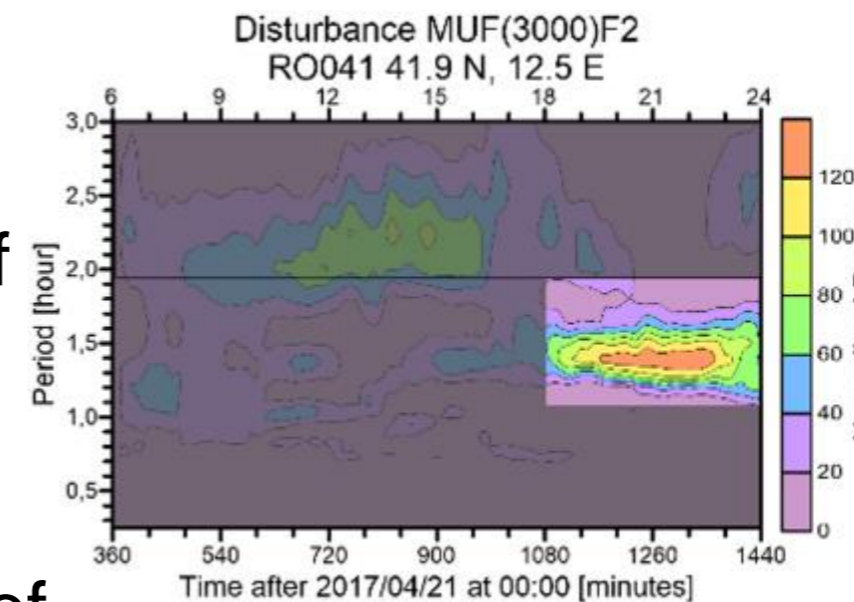
2.- Detection of TID-like variation

-Detect coherent TID-like variations by spectral analysis. Periodograms calculation and search of the dominant period.

-TIDs contribution to data variability. Application of the Parseval's relation

$$\sum_{n=-\infty}^{\infty} |x[n]|^2 = \frac{1}{2\pi} \int_{-\pi}^{\pi} |X(\omega)|^2 d\omega \sim \sum_{T=T_S}^{T=T_E} A(\omega)^2$$

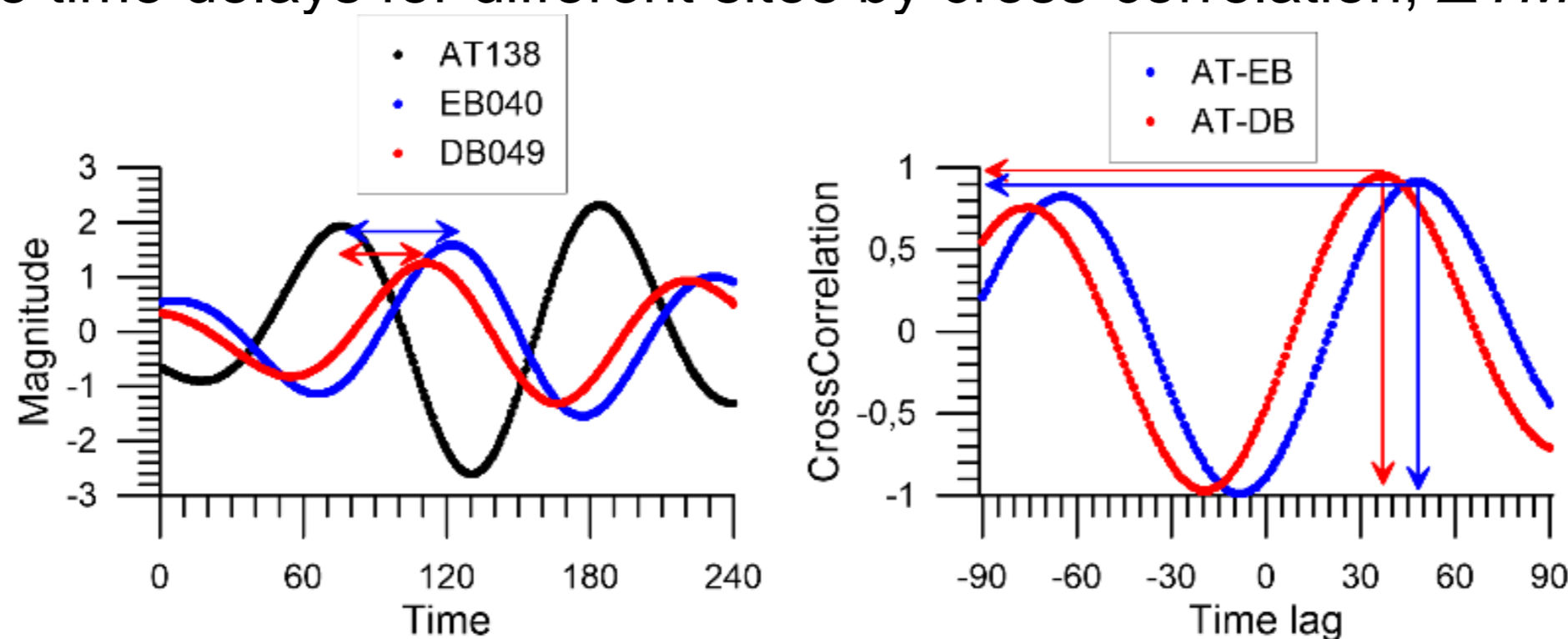
$$SEC(\%) = \frac{\sum_{T=T_{TID_S}}^{T=T_{TID_E}} A(T)^2}{\sum_{T=T_S}^{T=T_E} A(T)^2}$$



HF-Interferometry (HFI) method

3.- Estimation of the velocity and azimuth of the TID

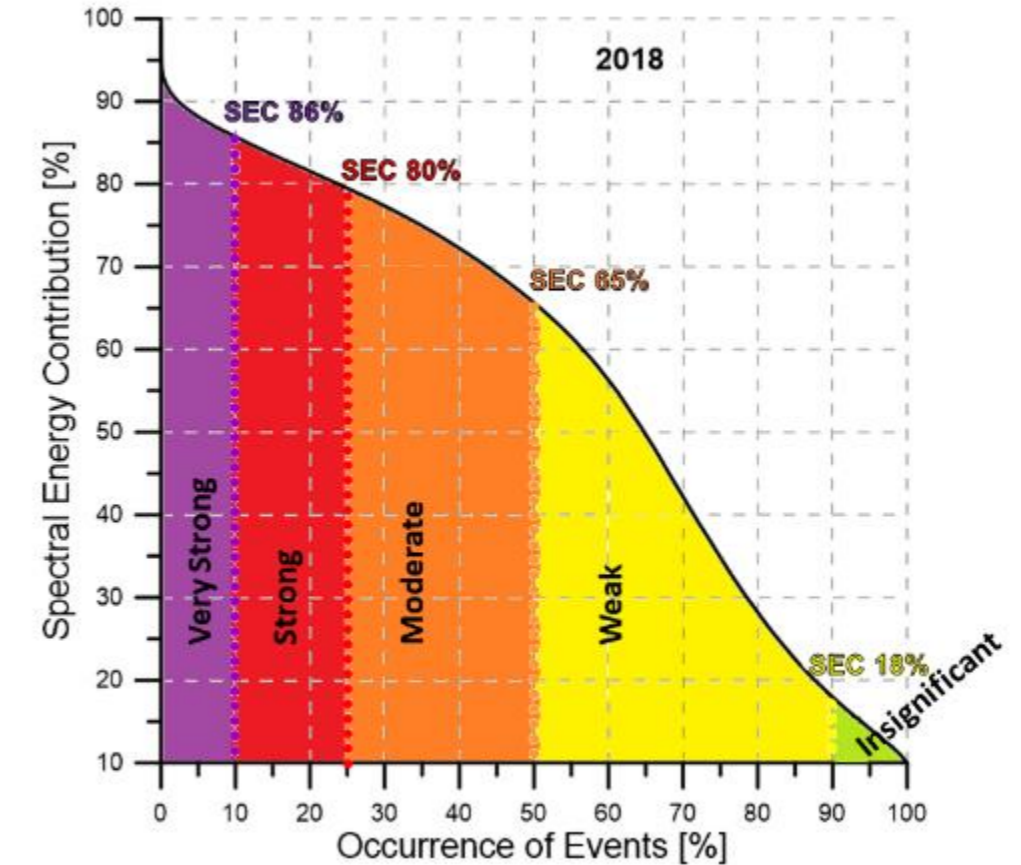
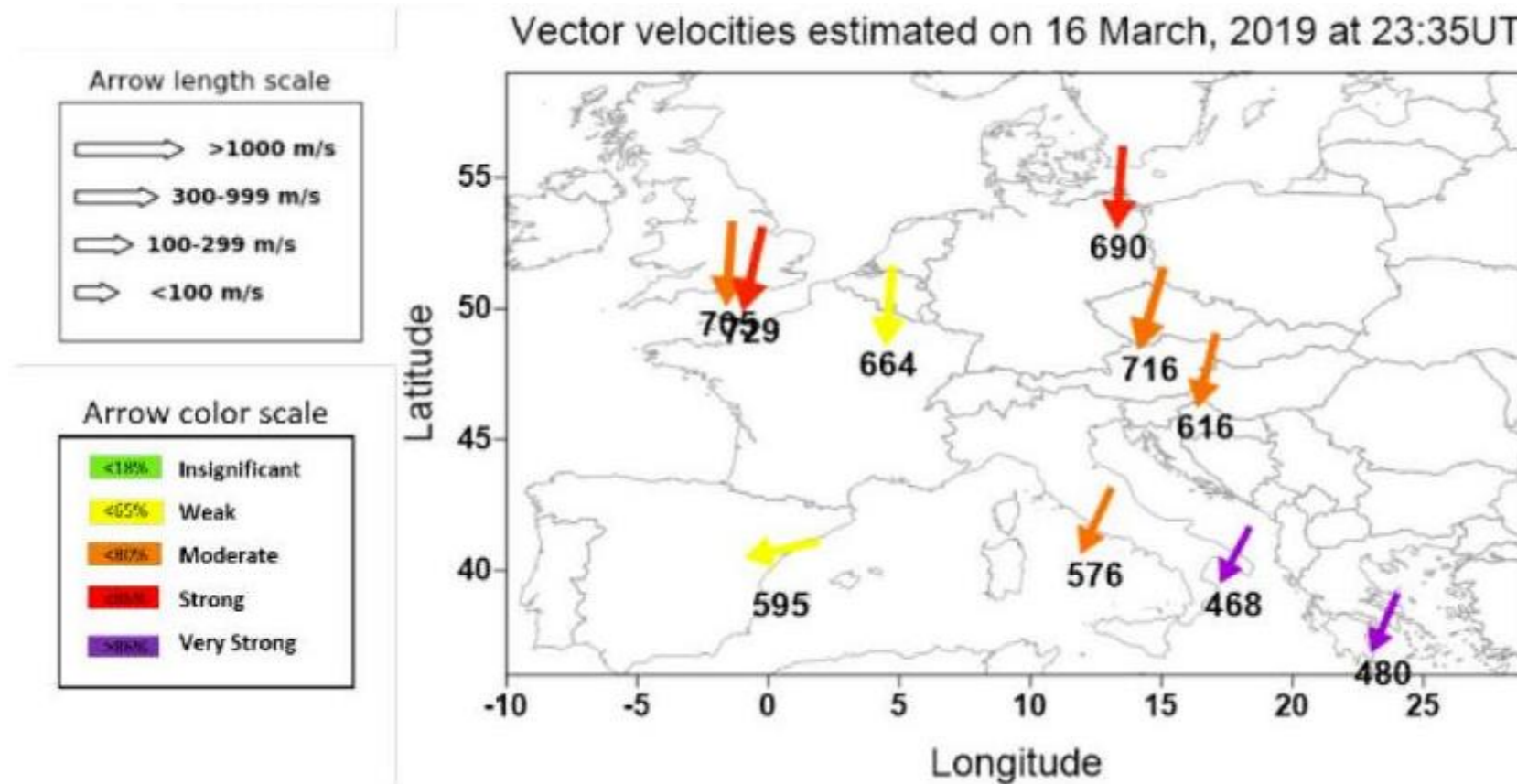
- Estimate time delays for different sites by cross-correlation, ΔTM_i



- Estimate velocity of disturbance \vec{v} assuming planar propagation.

$$\Delta TM_i - \vec{s} \cdot \Delta \vec{r}_i = 0 ; \quad \vec{v} = \frac{\vec{s}}{s^2} .$$

HF-Interferometry (HFI) method: Products



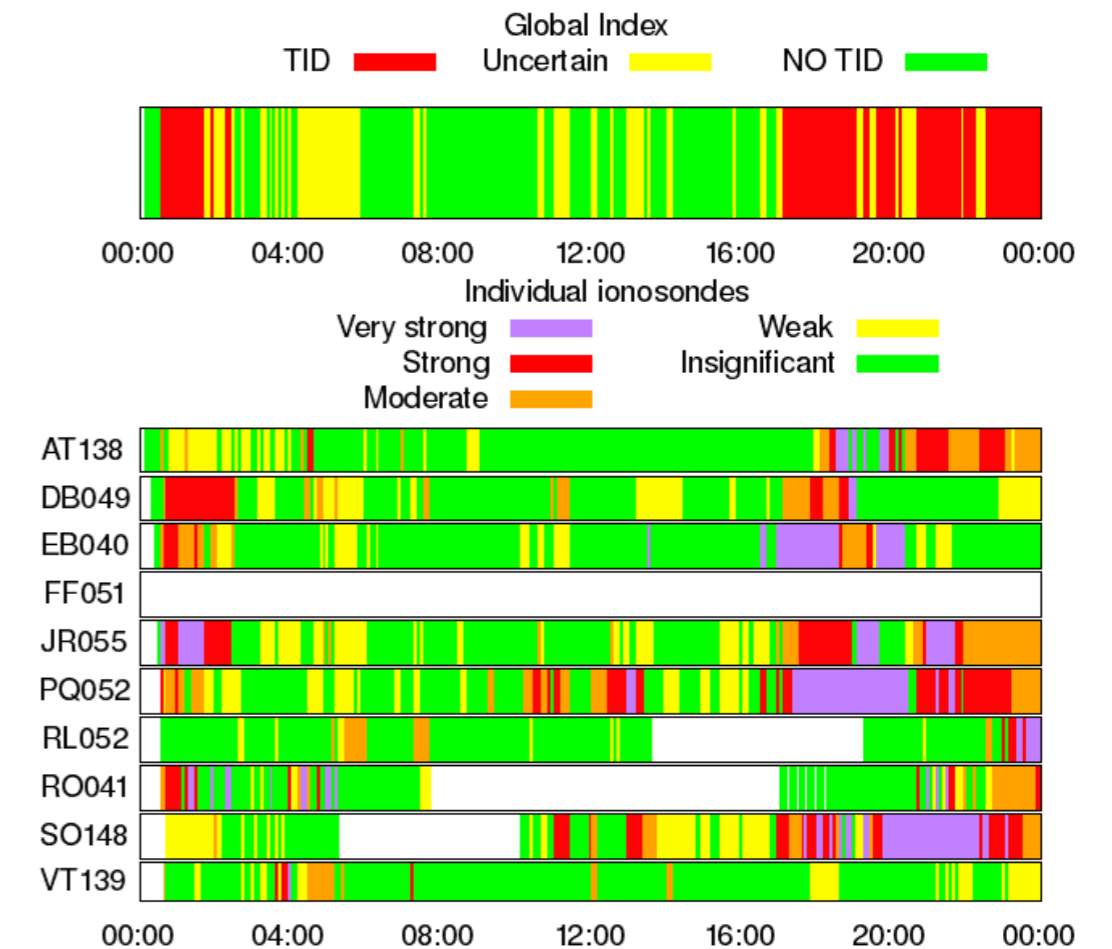
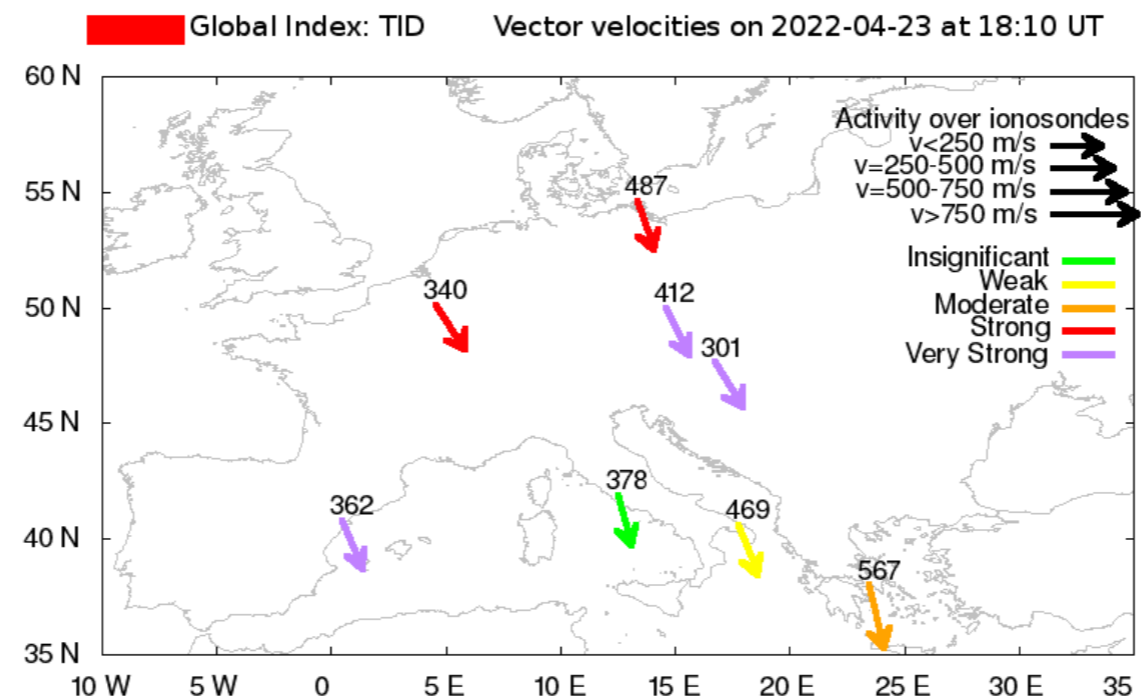
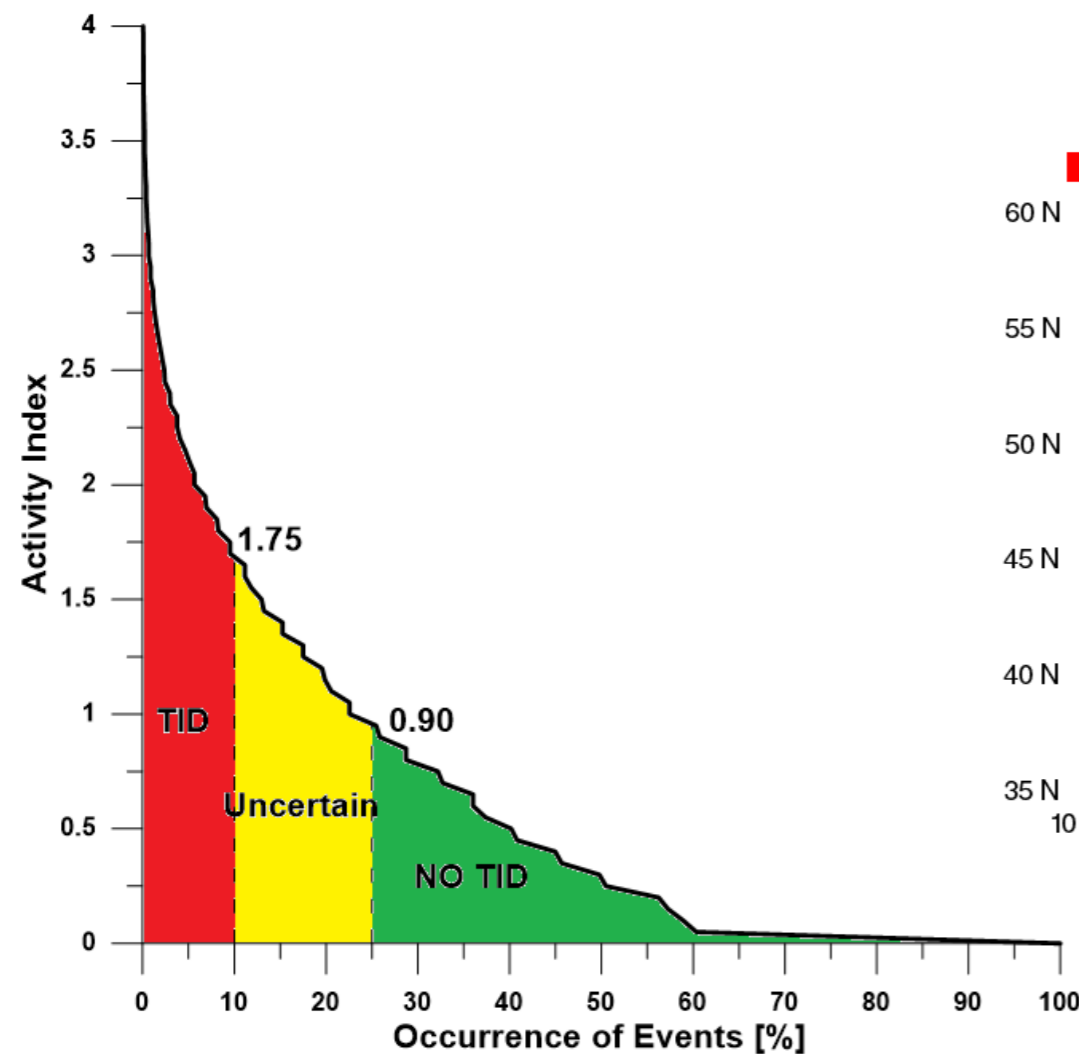
TechTIDE project Ebre Observatory HF-Interferometry

NT	ST	FL	STA	DATE&TIME	ALATI	ALONG	NW	IW	PERIO	POWER	AMPLI	SPCONT	VEL	AZI	TrL	IQ	IR
1	1	1	AT138	201903162335	38.00	23.50	2	1	121	46.3	0.15	86.8	480	204	5	100	88
1	2	1	DB049	201903162335	50.10	4.60	2	1	115	124.1	0.55	62.3	664	185	2	100	44
1	3	1	EB040	201903162335	40.80	0.50	2	1	98	36.3	0.25	24.1	595	239	2	100	77
1	4	1	FF051	201903162335	51.70	-1.50	2	1	124	94.6	0.15	78.2	705	183	3	100	66
1	5	1	JR055	201903162335	54.60	13.40	2	1	140	94.1	0.19	81.6	690	181	4	100	66
1	6	1	PQ052	201903162335	50.00	14.60	2	1	116	108.2	0.49	65.4	716	197	3	100	88
1	7	1	RL052	201903162335	51.50	-0.60	2	1	138	55.4	0.27	80.2	663	191	4	100	55
1	8	1	R0041	201903162335	41.90	12.50	2	1	122	113.7	0.70	77.9	576	204	3	100	100
1	9	1	S0148	201903162335	47.63	16.72	2	1	129	83.7	0.47	70.8	616	191	3	100	100
1	10	1	VT139	201903162335	40.60	17.80	2	1	142	156.9	0.74	91.7	468	209	5	100	77

HF-Interferometry (HFI) method: Products

Activity index:

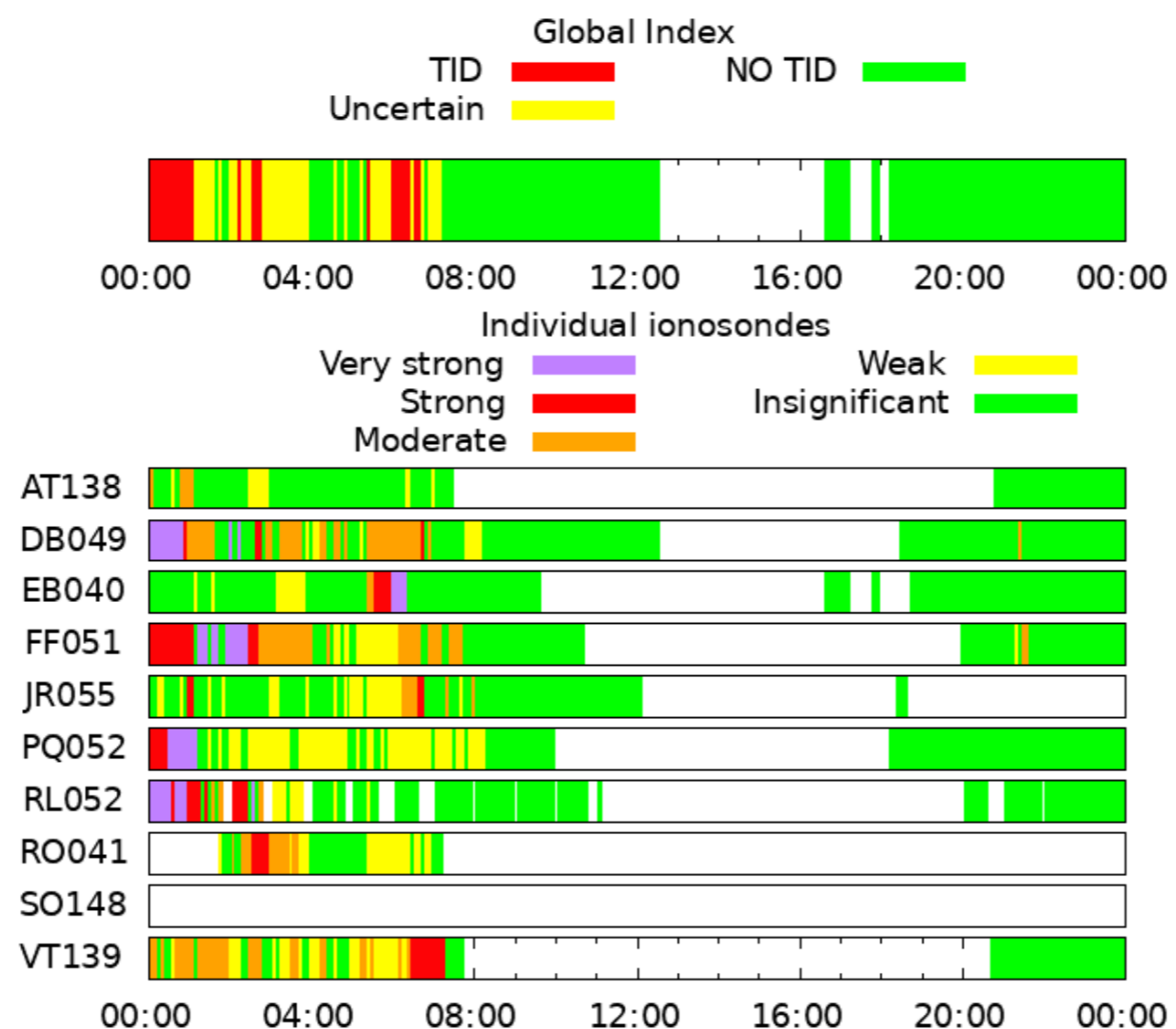
Defined as the product of the average of assigned numbers (1 to 5) for each ionosonde according to its SEC and the area affected



HF-Interferometry (HFI) method: Problems/Limitations

The method has been running continuously in near real time since April 2019.

The main issues experimented since then is the scarcity of data during summertime because the presence of Sporadic E layer, Es



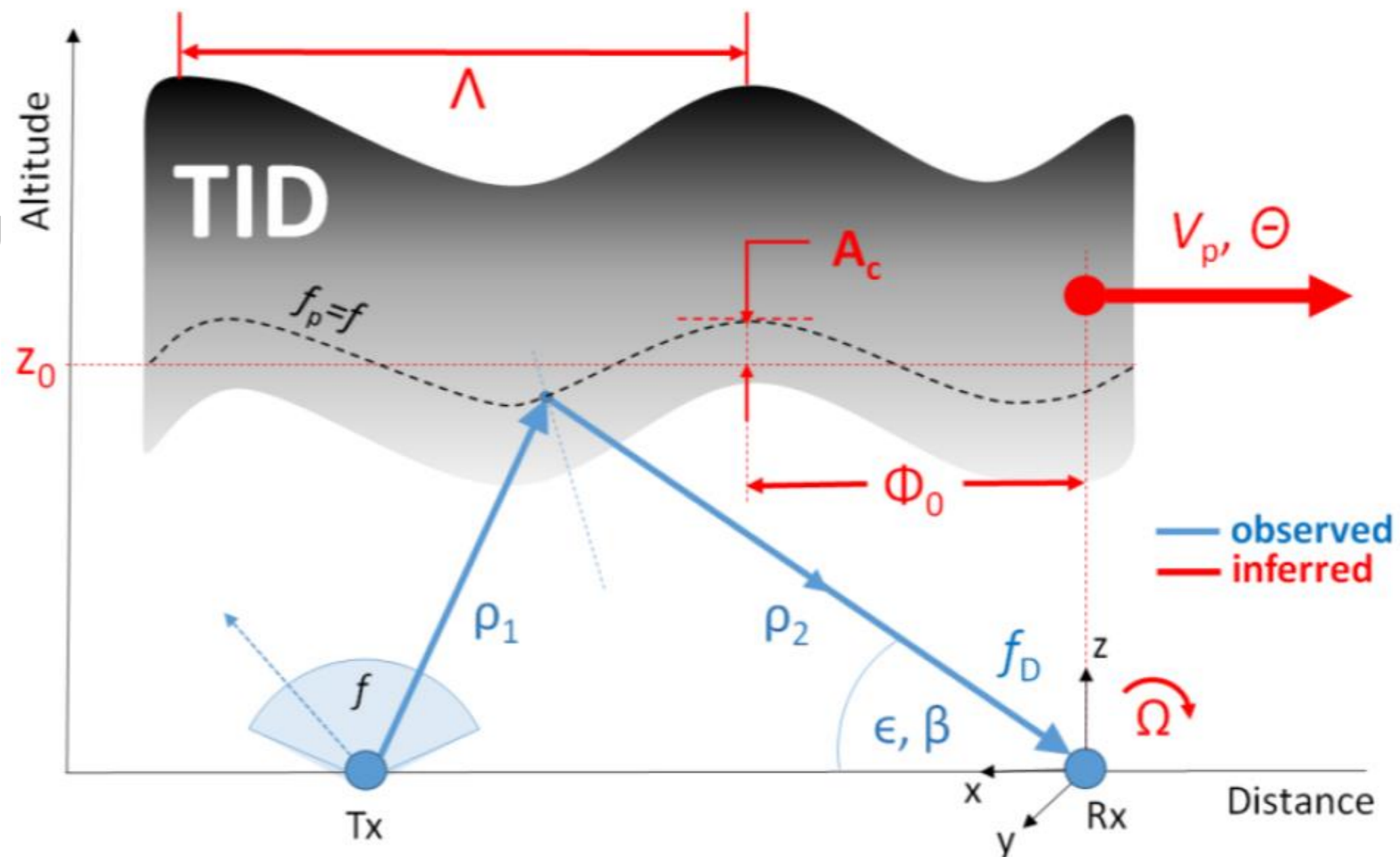
HF-TID method

IdN. Method	Main Characteristics	Intermediate Product	Final Product	Value added Product
HF-TID Detects perturbations in space from all possible sources (solar and lower atmosphere origin) and it is suitable for the identification of both MS and LS TIDs	<u>Input</u> : signal properties from Digisonde synchronized operation. <u>Output</u> : TID velocity, amplitude, propagation direction at the signal reflection point between the stations	Doppler frequency, angle of arrival, and time-of-flight from Tx to Rx, both OI and VI sounding	Separately for MS and LS TID: 1+ detections of {TID Period, Phase Velocity, Direction of propagation, Wavelength, and Amplitude}	Maps of the current TID activity Maps of TID occurrence probability

HF-TID method

HF-TID is sensitive to the quasi-periodic variations of the HF signal recorded on an oblique D2D link [Reinisch et al. 2018].

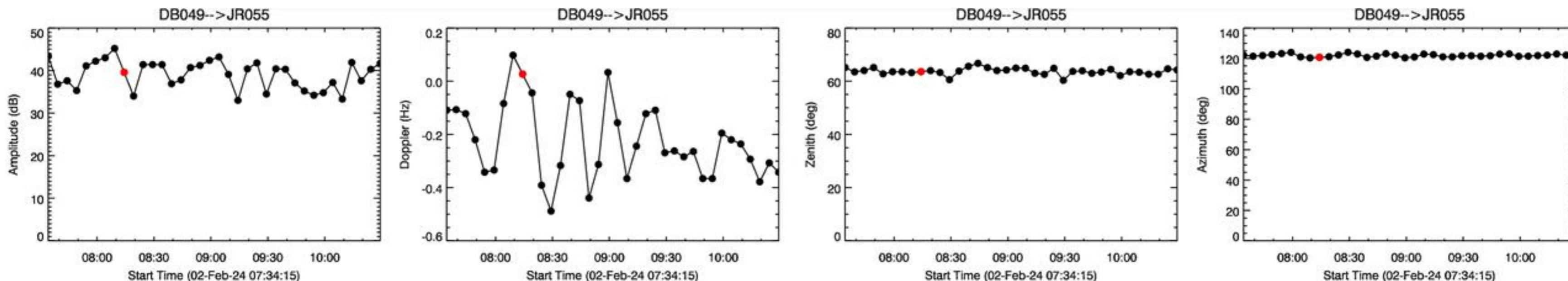
In a simple case of one wave-like traveling disturbance of amplitude A and wavelength Λ , propagating horizontally with a phase velocity V_p and travel azimuth Θ , the HF radio signal that traverses the ionospheric channel exhibits distinct oscillating patterns of the temporal variation of its properties: Doppler frequency $\delta(t)$, angles of elevation $\varepsilon(t)$ and azimuth $\beta(t)$, and time-of-flight $\tau(t)$ [Huang et al. 2016].



HF-TID method

HF-TID associates the *observed* signal variations of $\varepsilon(t)$, $\beta(t)$, $\delta(t)$, and $\rho(t)$ at the dominant TID wave angular frequency Ω with the *underlying* TID phenomenon defined by A , Λ , V_p , and Θ . The TID wave amplitude A_N is one of derived properties. A_N is defined formally under assumption of a simple TID model in which, for any fixed altitude z_0 in the ionosphere, TID is a sinusoidal perturbation of the background density $N_0(x, y, z_0, t)$ in time t and horizontal plane (x, y) :

$$N(x, y, z_0, t) = N_0(x, y, z_0, t) \left[1 + A_n(z_0) \cos \left(\Omega t - \frac{2\pi}{\Lambda} \vec{r} \right) \right]$$



HF-TID method

To determine the dominant Ω value, HF-TID first calculates the spectrum S_δ by running a Discrete Fourier Transform (DFT) on the Doppler frequency variation $\delta(t)$. The frequency Ω at which $S_\delta(\Omega)$ has its maximum value over all computations is selected as the dominant TID wave frequency.

At this selected Ω , the FFT operation is then applied over the elevation angle $\varepsilon(t)$ and the azimuth angle $\beta(t)$ to obtain $S_\varepsilon(\Omega)$ and $S_\beta(\Omega)$ respectively.

Finally, the TID model parameters A , Λ , V_p , and Θ are obtained as:

$$A_N = iS_\delta(\Omega) \frac{\lambda}{2\Omega z_0 \sin \varepsilon_0}$$

$$K = \frac{2\pi}{\Lambda} = -\frac{2\Omega \operatorname{Im} S_\beta \cos \varepsilon_0}{\lambda \operatorname{Im} S_\delta \sin \Theta}$$

$$\tan \Theta = -\frac{2z_0 \Omega \operatorname{Re} S_\beta}{2z_0 \Omega \operatorname{Re} S_\varepsilon \tan \varepsilon_0 + \lambda \operatorname{Im} S_\delta \sin \varepsilon_0}$$

$$V_p = \frac{\Omega}{K}$$

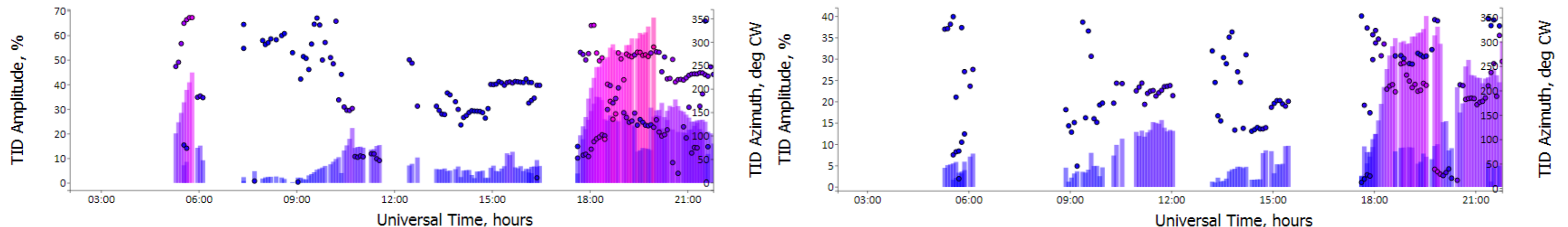
FAS technique, Paznukhov et al. 2012

HF-TID method

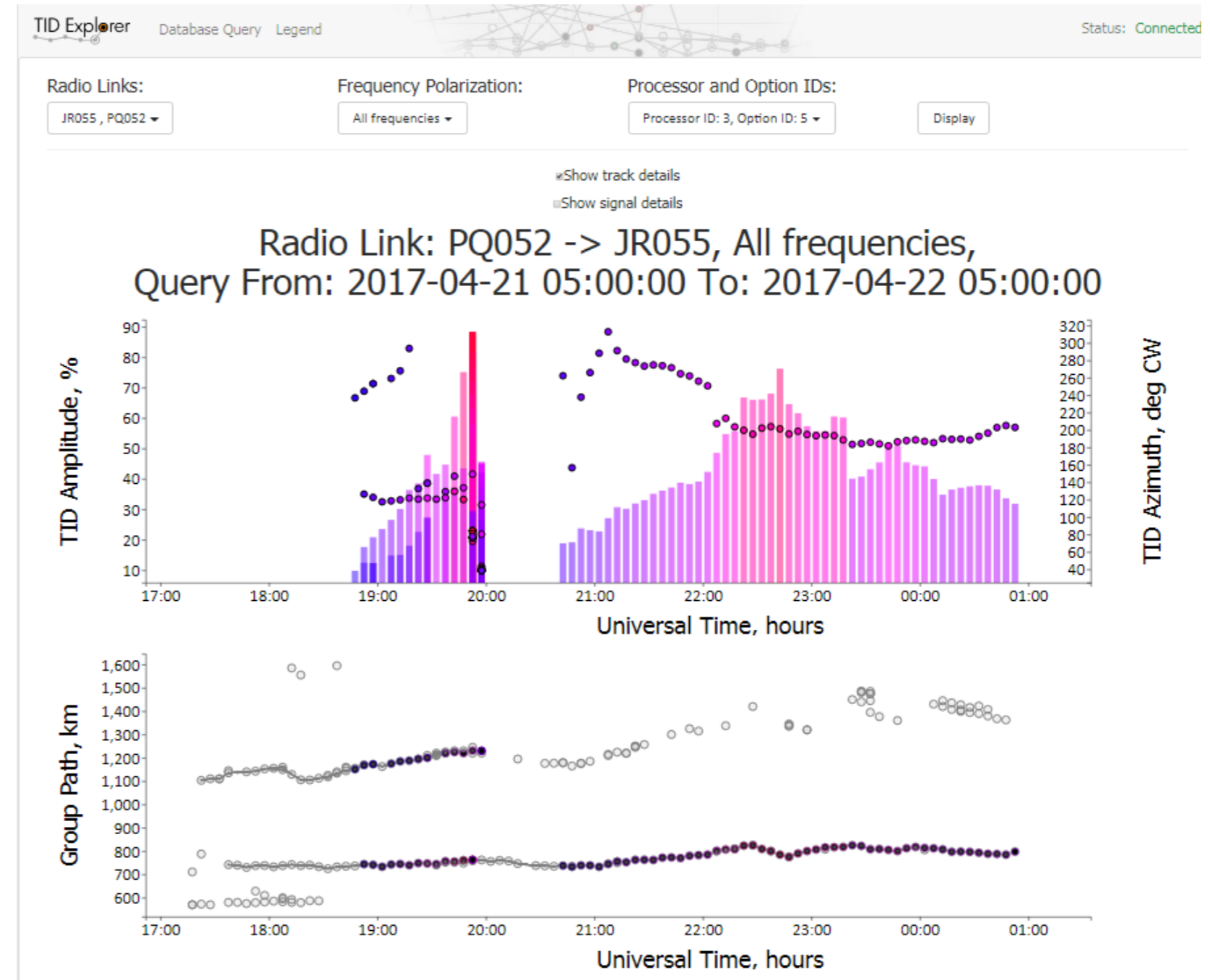
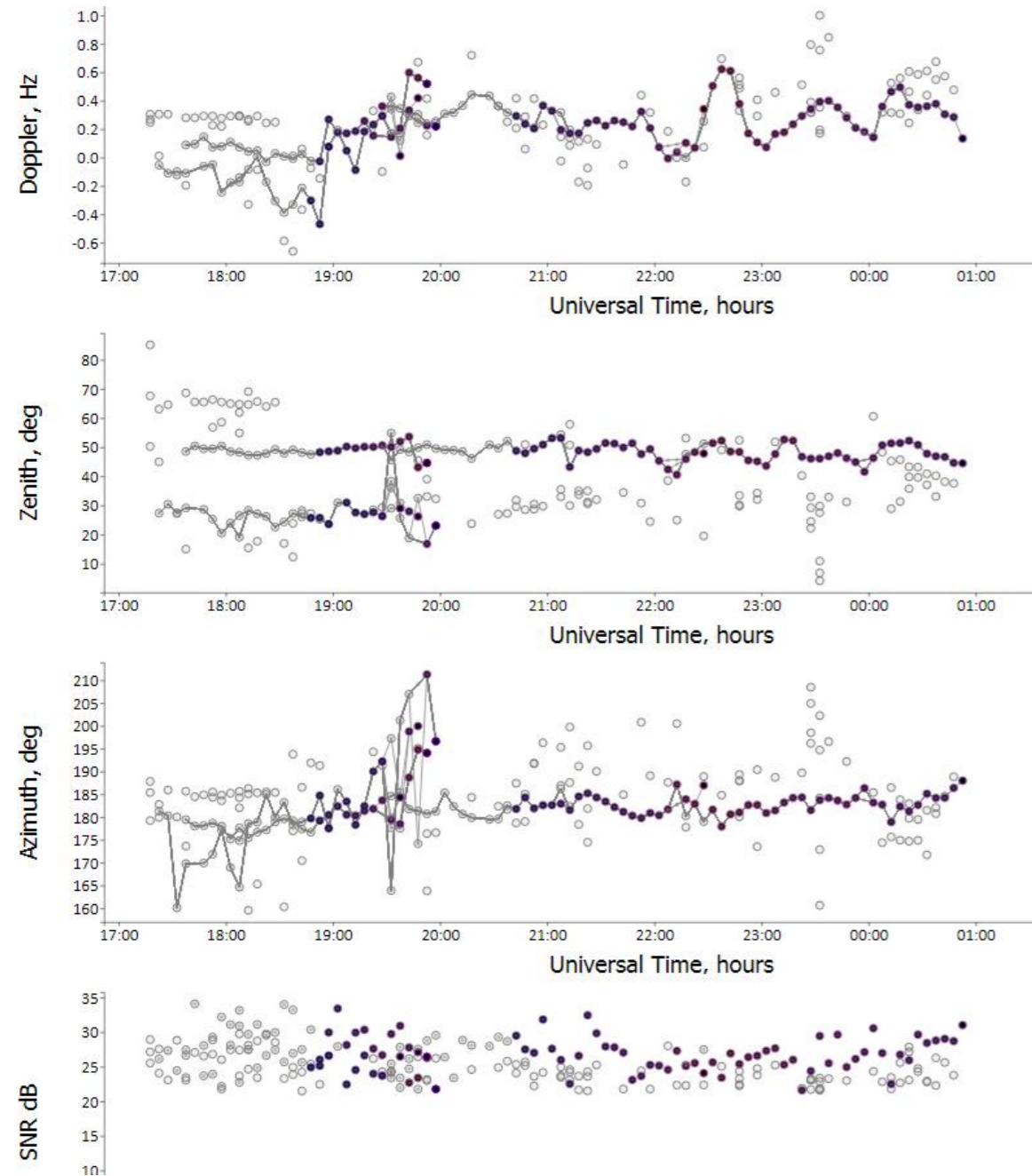
Once, HF-TID determines the angular frequency Ω and the wavelength Λ , the direction of propagation of the TID in the horizontal plane, Θ is:

$$\vec{r} = x \cos \Theta + y \sin \Theta$$

The perturbation amplitude $A_N(z_0)$ is an excellent candidate for a consistent and objective characterization of the TID phenomenon. For an easier interpretation, $A_N(z_0)$ is given in %:

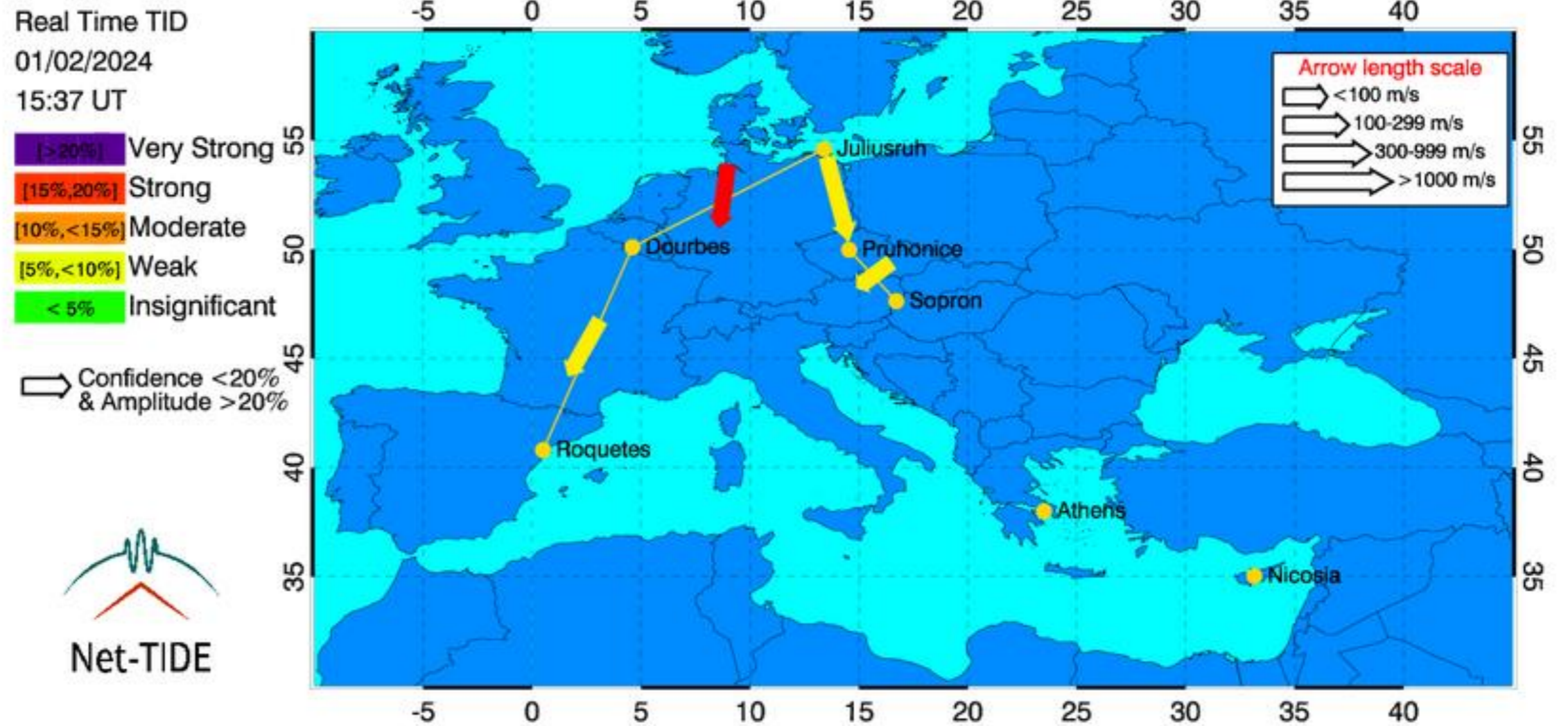


HF-TID method



HF-TID method: Products

Net-TIDE

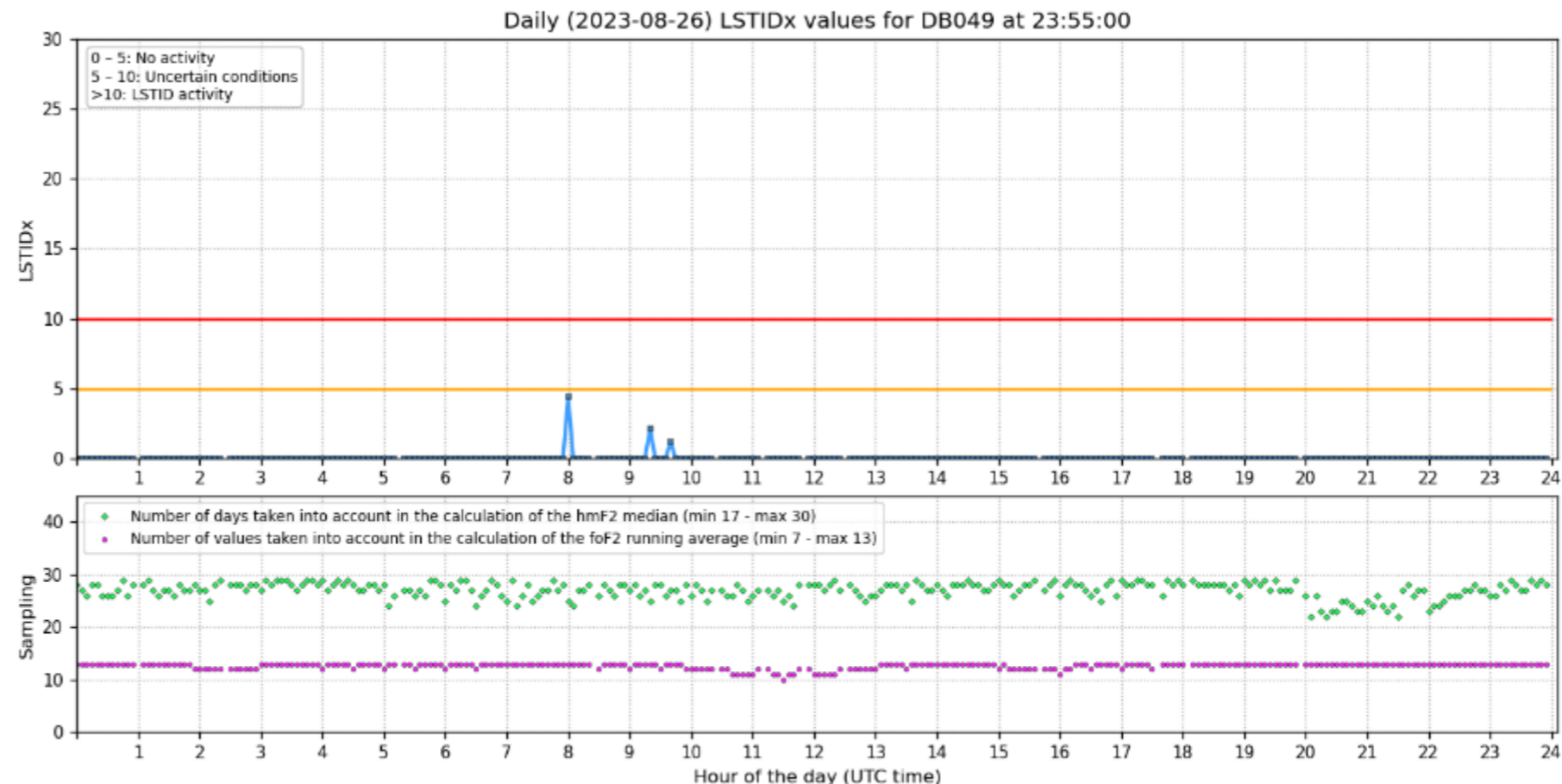


LSTIDx index

IdN. Method	Main Characteristics	Intermediate Product	Final Product	Value added Product
3D EDD Maps Analyze maps of TEC and ionospheric characteristics and it is sensitive to perturbation from LSTIDs only.	Input: ionospheric characteristics at the hmF2 altitude and TEC maps. Output: Analytical function of the electron density distribution with altitude from 90 km to 22000 km	1D electron density distribution (EDD) over the Digisonde locations	3D EDD results over a user-specified area. Maps of ED for vertical, horizontal and slant surfaces, specified by the user.	Maps of gradients of the integrated electron density for altitudinal ranges defined by the user.

LSTIDx index

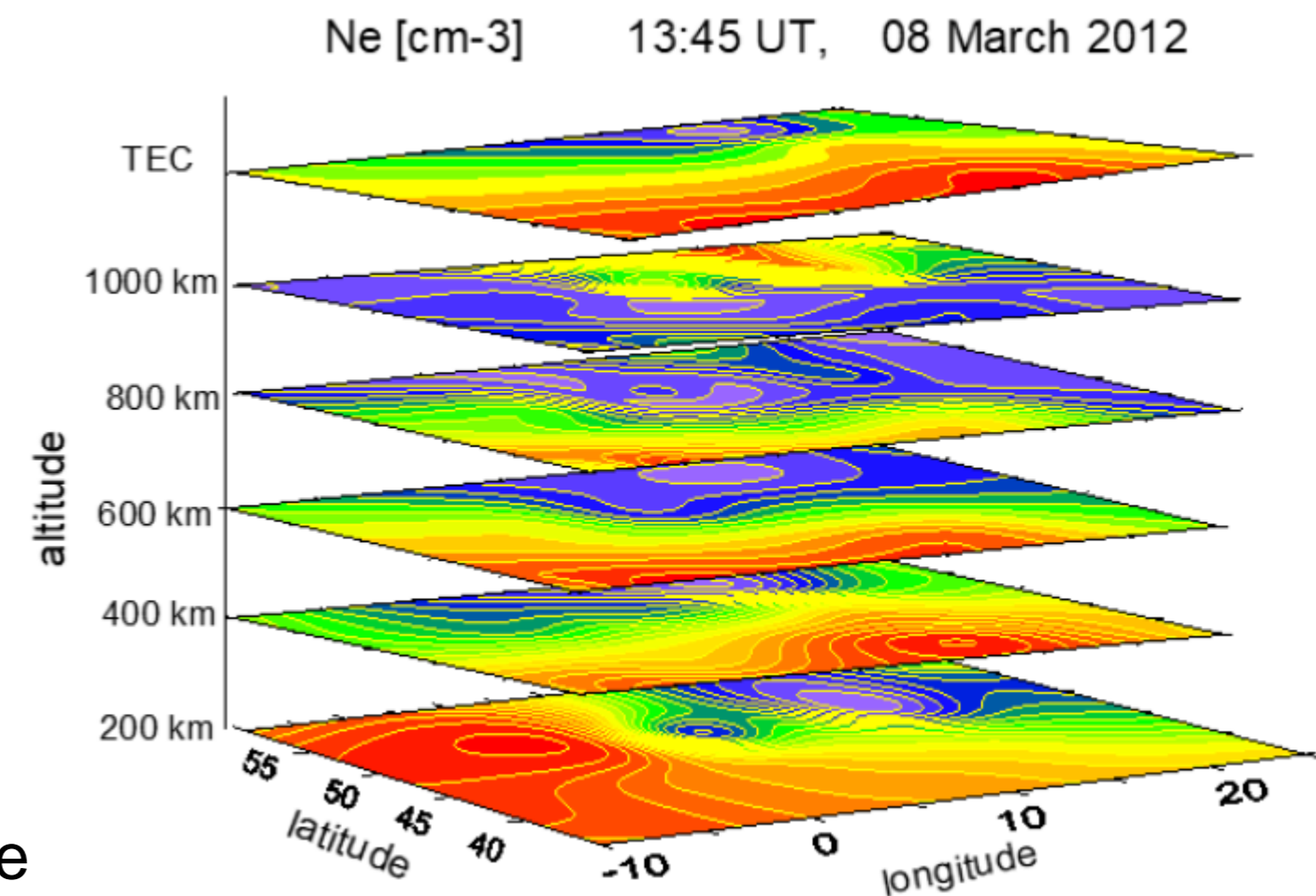
The LSTID index is the maximum value of the running relative standard deviation (RSTD%) of the electron density within 1 hour over 12 data points, at any ionospheric height from 150 to 600 km. The electron density is calculated with the **TaD model** [Kutiev et al. 2016; Belehaki et al. 2016], which provides the reconstructed electron density from the bottomside ionosphere up to the plasmasphere using the empirical model derived from the Alouette/ISIS topside sounders data, the **ionospheric characteristics at hmF2** obtained from an ionospheric sounder and with the **TEC parameter** at the location of the ionospheric sounder.



LSTIDx index

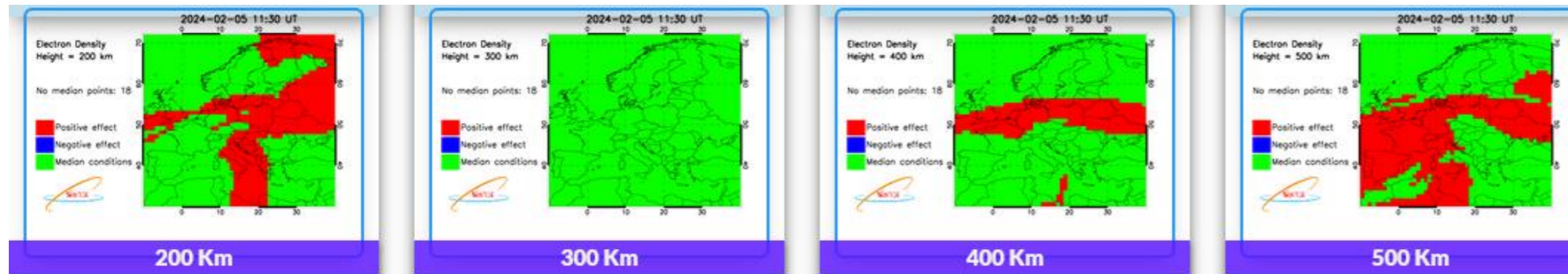
TaD model:

- the Topside Sounders Model (TSM), that provides the empirical functions for the O⁺- H⁺ transition height (hT), the topside electron density scale height (HT) and their ratio $R_t = HT/hT$, derived from the Alouette/ISIS data;
- the Topside Sounders Model Profiler (TSMP) that offers analytical formulas for obtaining the shape of the vertical plasma distribution in the topside ionosphere and plasmasphere based on TSM parameters and on the F layer maximum density (NmF2), its height (hmF2) and its scale height (Hm) at its lower boundary, derived from Digisondes.
- the final TaD that performs the necessary transformations to the Digisonde autoscaled scale height so that the integrated TSMP electron density from the F layer peak to GNSS orbits can be finally adjusted to the measured GNSS TEC at the Digisonde location



Electron density maps over Europe at different altitudes (3D) resulted from the TaD model

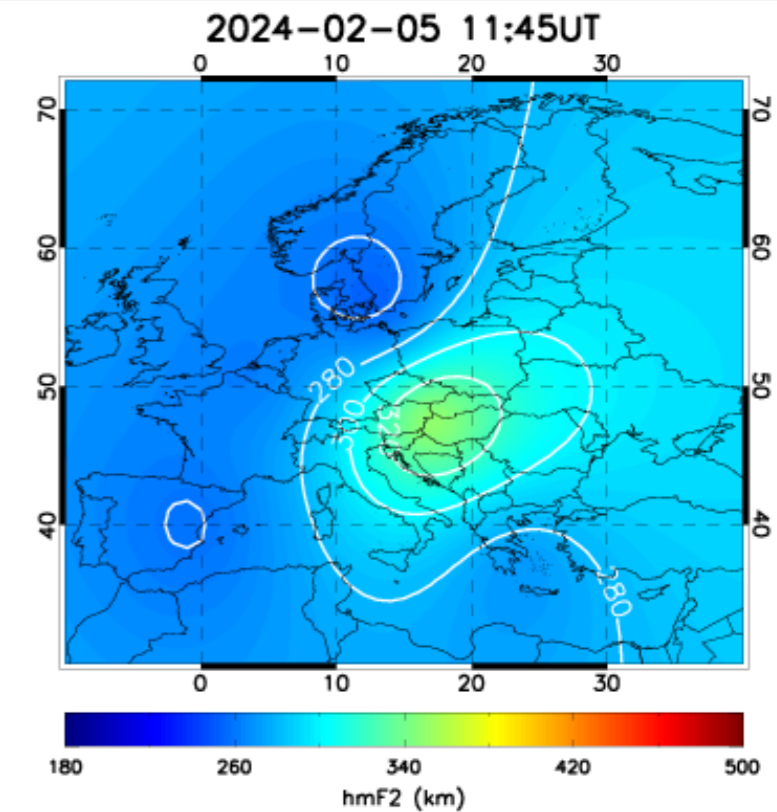
hmF2



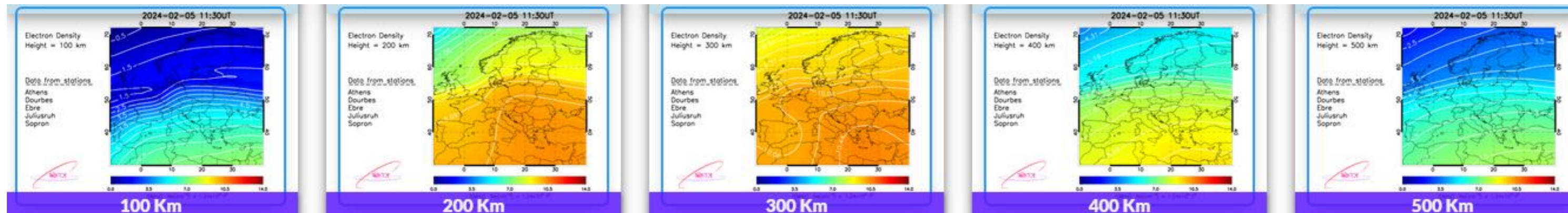
Maximum ionization height (hmF2)

Data from stations

Athens
Dourbes
Ebre
Juliusruh
Sopron



foF2



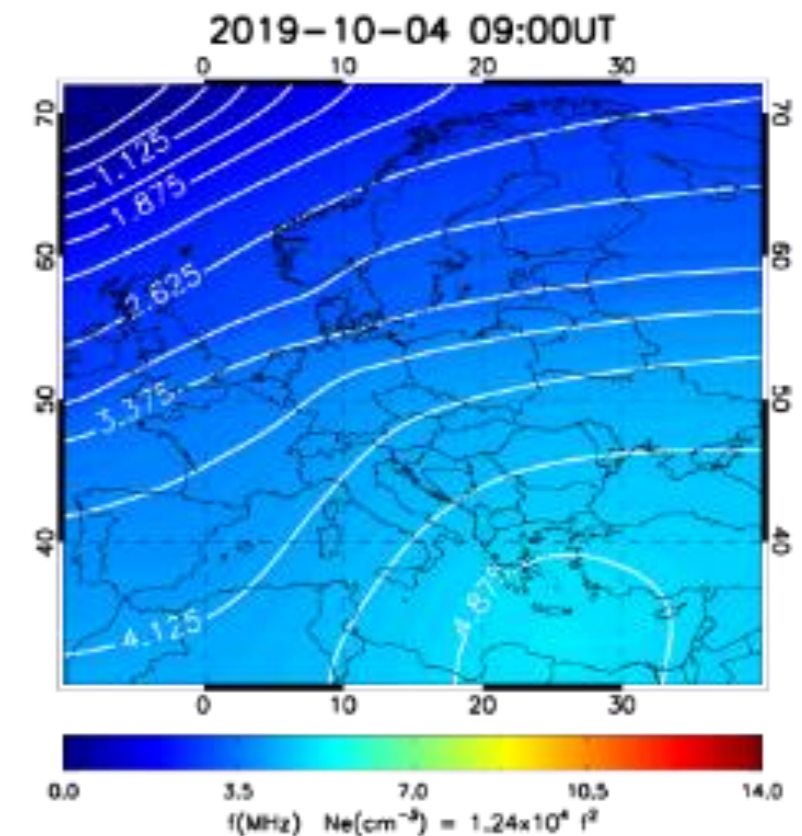
3D EDD Maps method:

Background ionospheric conditions

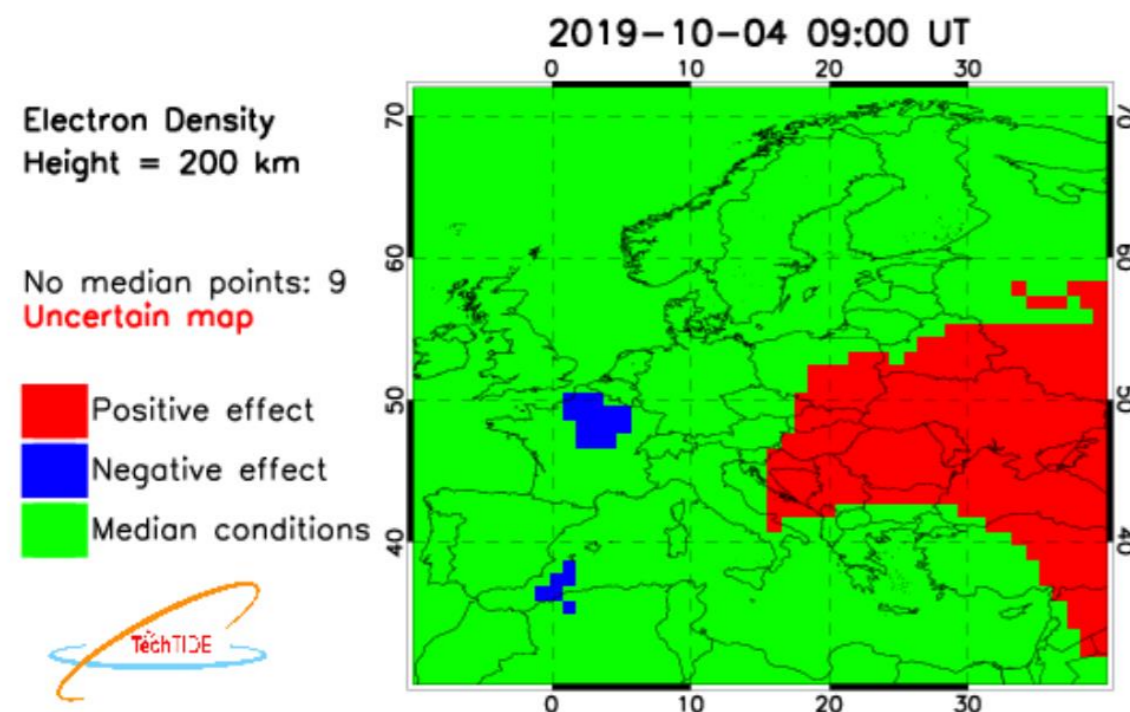
- $|dN_e| < 1\sigma$ median conditions
- $dN_e > 1\sigma$ positive
- $dN_e < -1\sigma$ negative

Electron Density
Height = 300 km

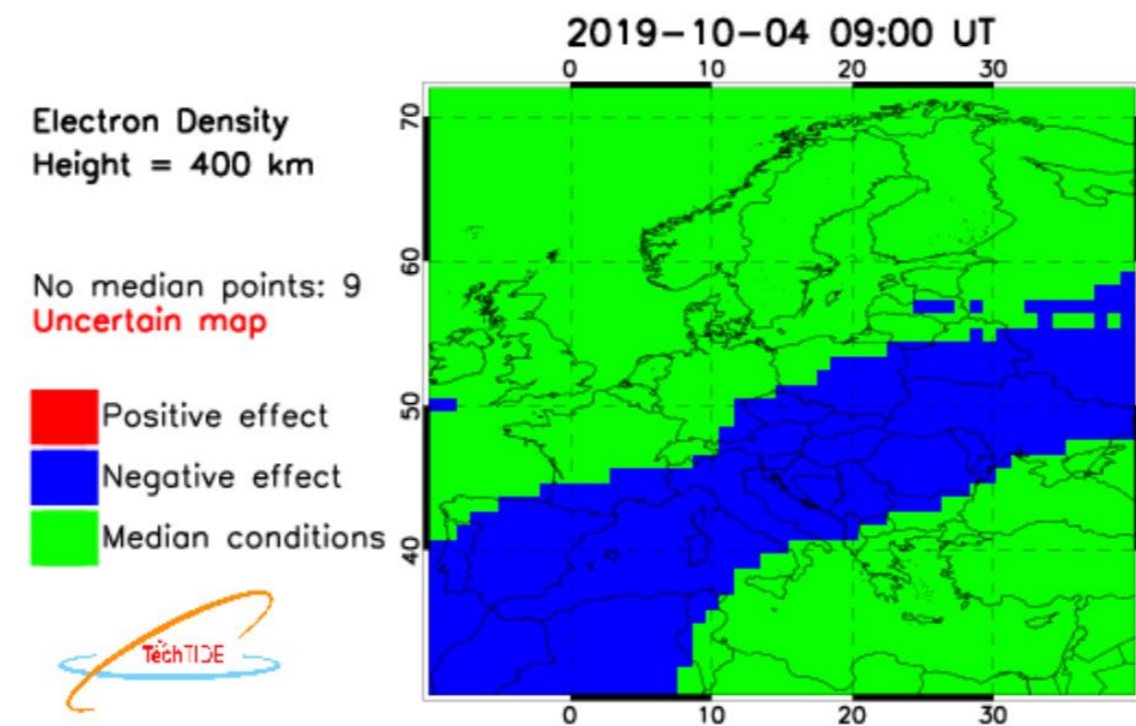
Data from stations
Athens
Dourbes
Ebre
Juliusruh
Pruhonice



Median conditions are dominating

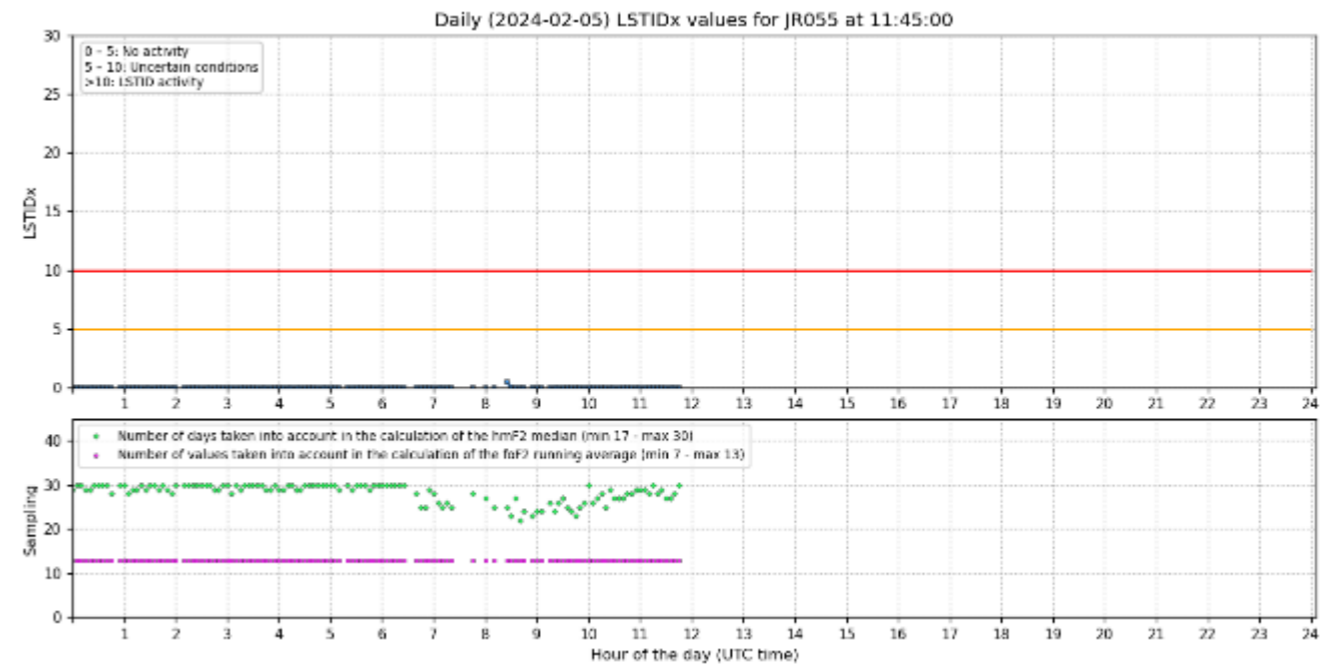
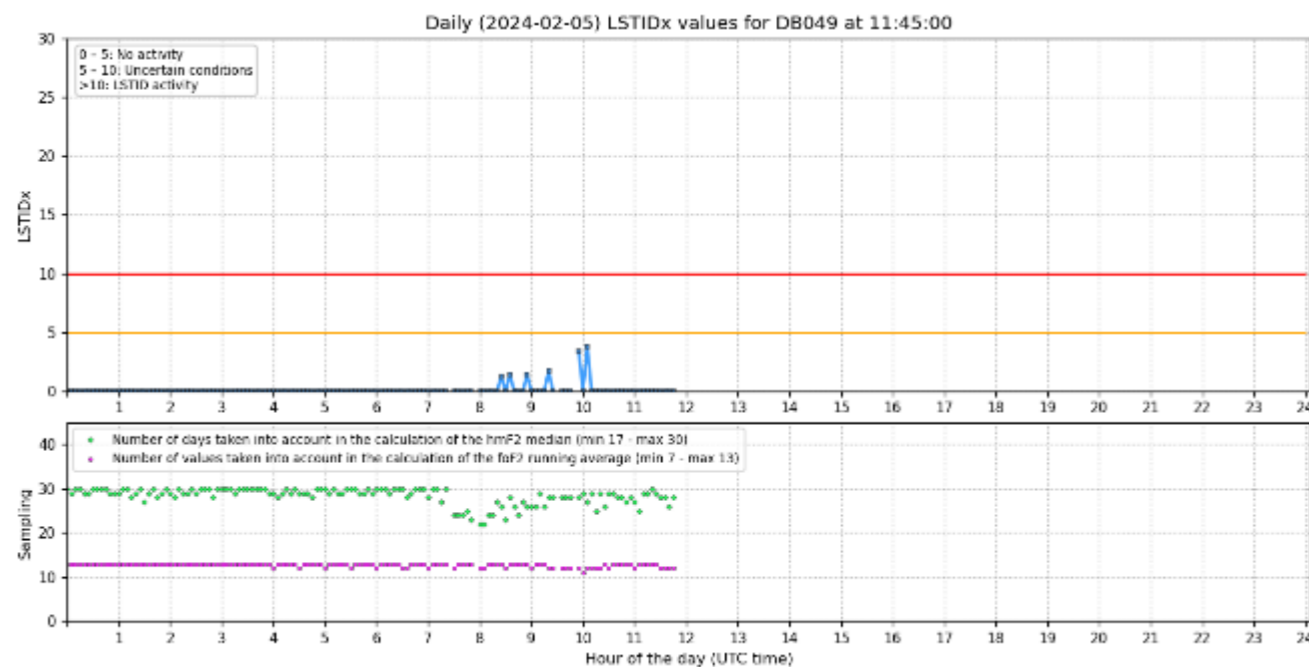
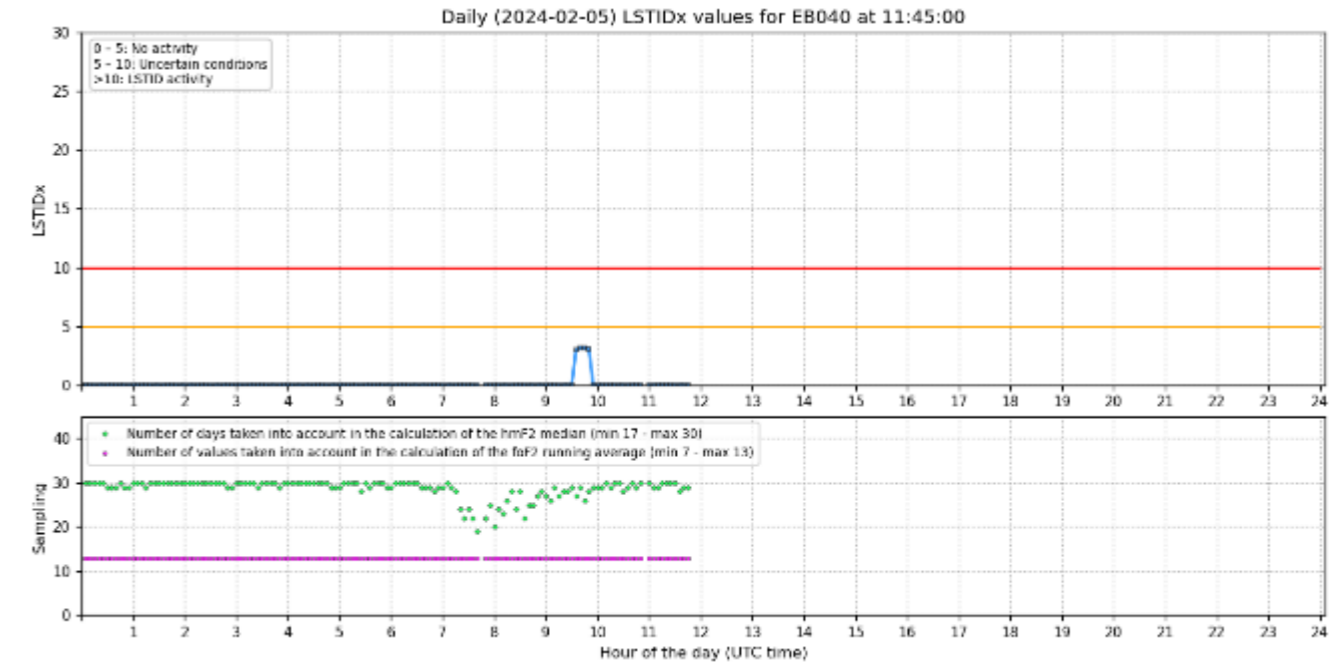
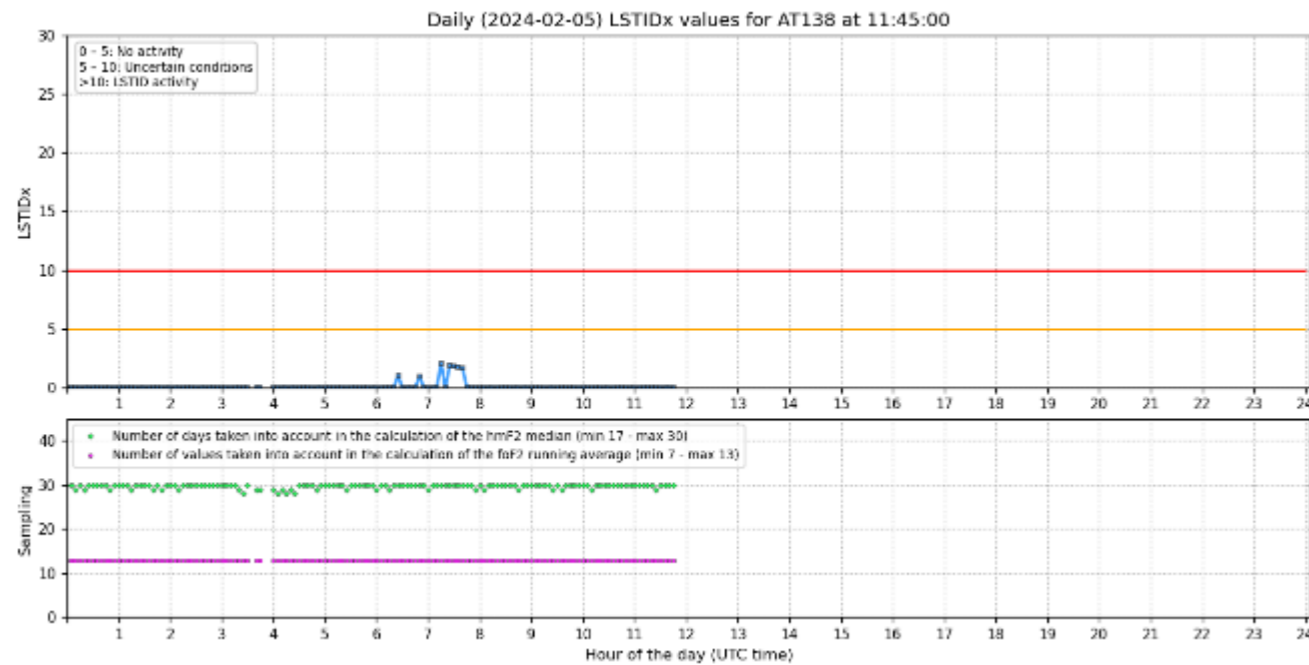


Conditions tend to be median



LSTIDx index

Maximum value of the running relative standard deviation (RSTD%) of the electron density.

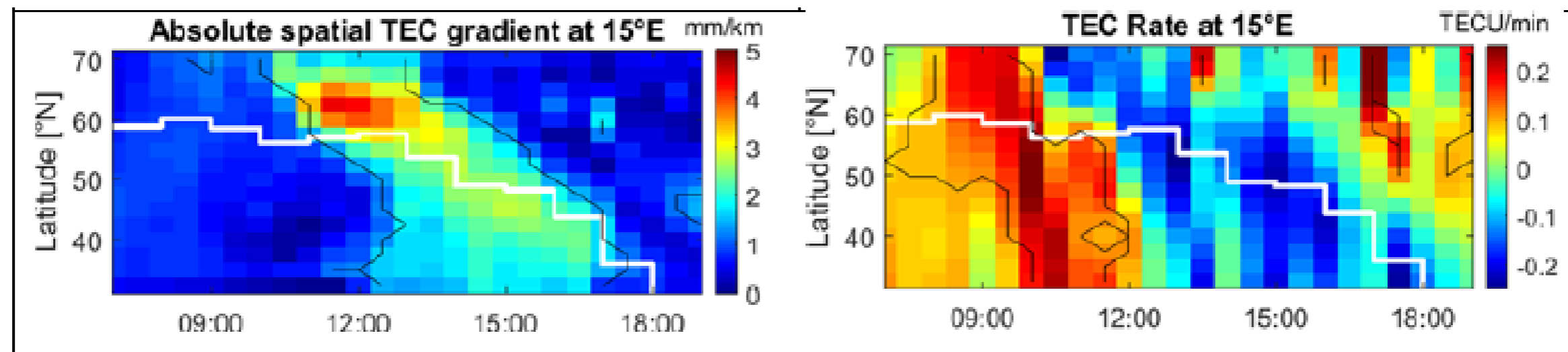


GNSS TEC Gradient method

IdN. Method	Main Characteristics	Intermediate Product	Final Product	Value added Product
<p>GNSS TEC Gradient Analyze TEC maps and it is mostly sensitive to perturbations from LSTIDs.</p>	<p><u>Input</u>: Grids of TEC maps over a region. <u>Output</u>: Latitude-time maps of TEC gradients and indication of significant gradients.</p>	<p>Maps of TEC and TEC rate</p>	<p>TEC Gradients</p>	<p>Graphical presentation in an image</p>

GNSS TEC Gradient method

GNSS TEC [Borries et al. 2017] gradients are not a direct measure of TIDs. Instead, TEC gradients are considered to be a precursor for LSTID activity. Strong ionosphere-thermosphere perturbations in high-latitudes, which are generating the LSTIDs, are considered to be reflected in significant TEC gradients. Such TEC gradients associated to the generation of LSTIDs are typically observed in the Auroral region. The comparison between the LSTID occurrence in the detrended TEC and the TEC gradients shows that significant TEC gradients occur in high-latitudes ($55\text{-}70^\circ\text{N}$) prior to the passage of LSTIDs in mid-latitudes.



GNSS TEC Gradient method

Input for this algorithm are NRT TEC maps for Europe, which are generated at DLR. TEC is given in a regular grid with fixed grid size with $1^\circ \times 1^\circ$ grid size in latitude and longitude. The TEC gradient is computed as difference between neighbouring grid points $d\text{TEC}/dd$ measured in $\text{TECU}/^\circ$. This value is converted to L1 range error per distance measured in mm/km , using the estimation $1\text{TECU} \sim 160\text{mm}$ and the distance in degree is converted to kilometers. This is the typical measure of TEC gradients used in aviation applications.

GNSS TEC gradient provide the following activity category for detecting disturbances:

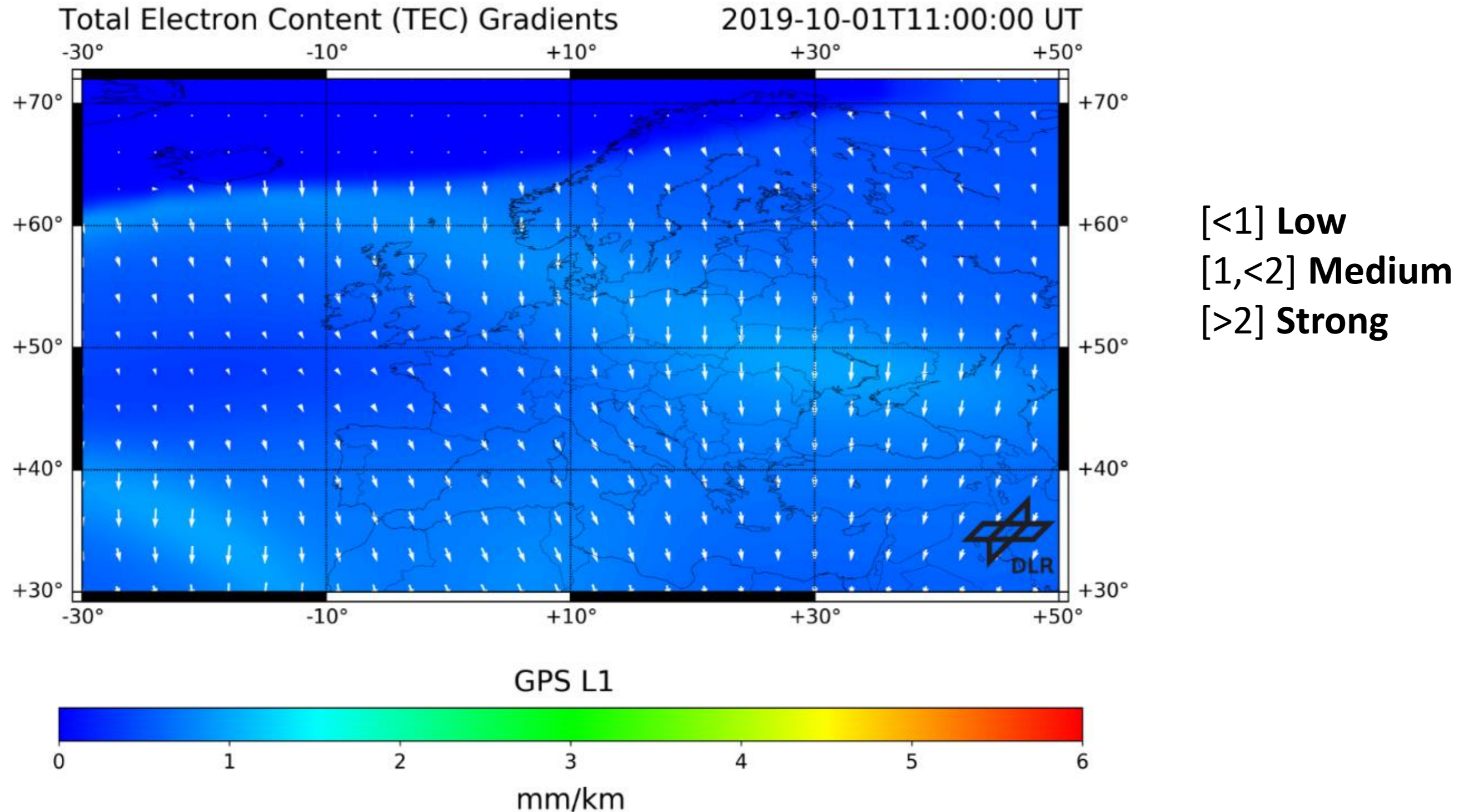
(|Amplitude|, expressed in mm/km):

Low category for $|\text{Amplitude}| < 1.2$,

Medium category for $1.2 \leq |\text{Amplitude}| < 2$,

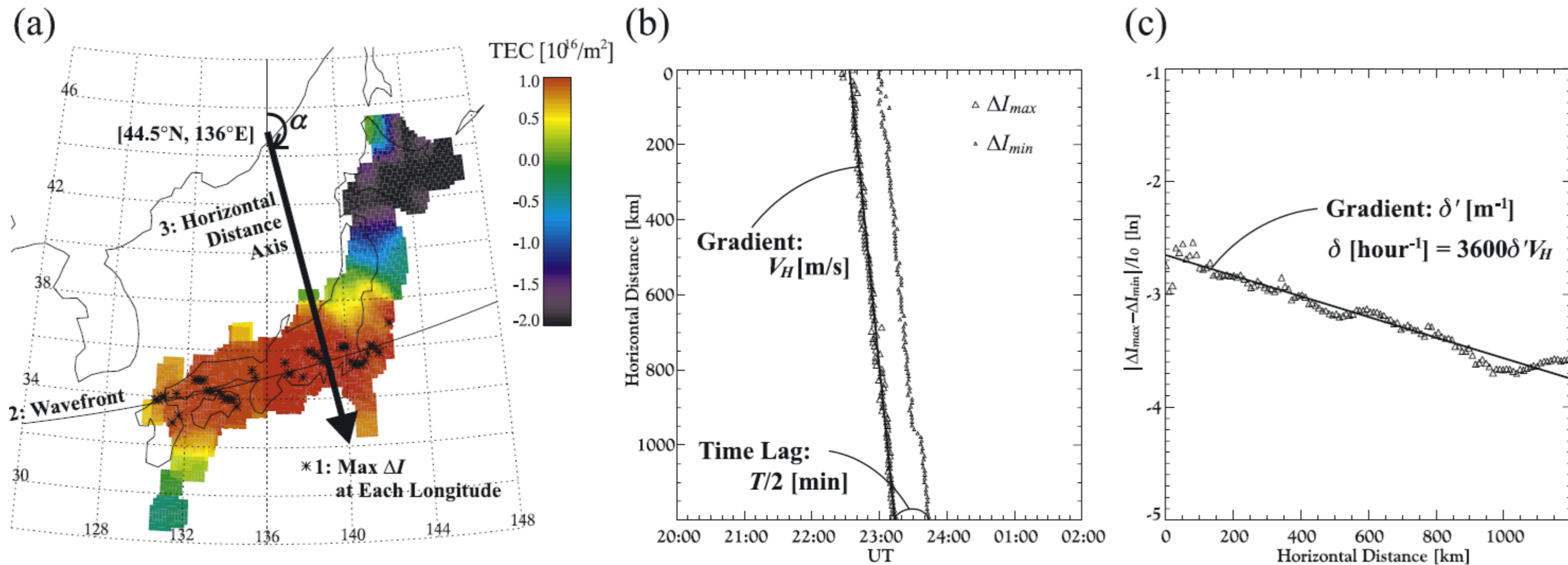
Strong category for $|\text{Amplitude}| \geq 2$.

GNSS TEC Gradient: TechTIDE Database (real time and archive)



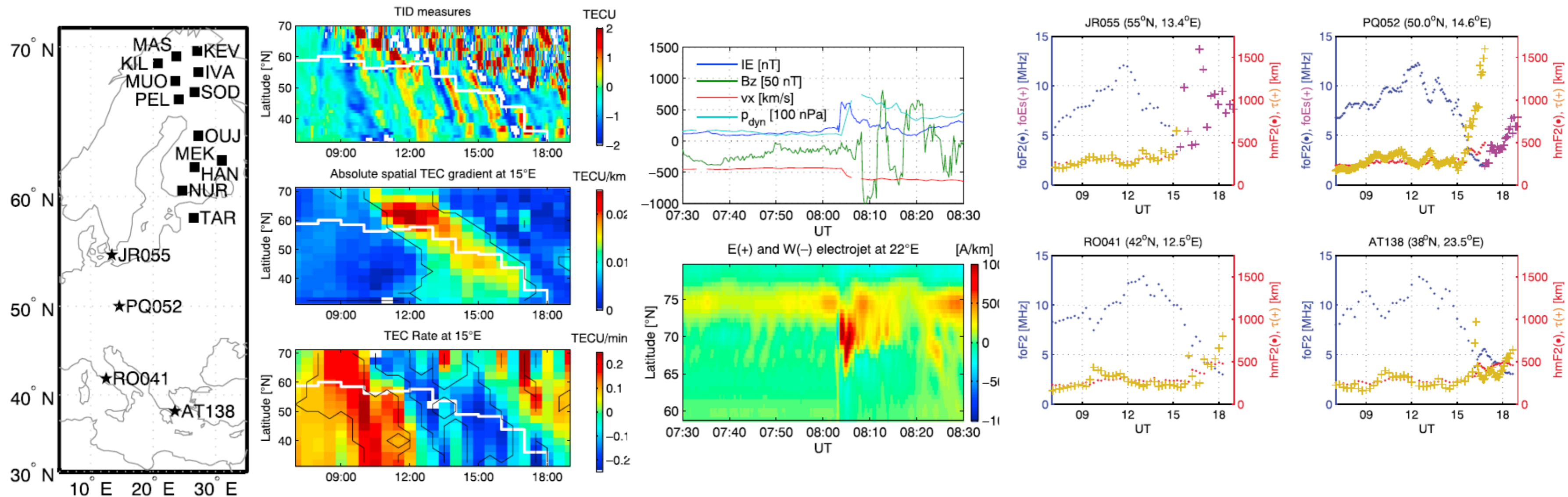
Tsugawa et al. 2004

Using total electron content (TEC) data from the GPS Earth observation network (GEONET), about 1000 GPS receivers and provides GPS data at every 30 s. High-resolution TEC time sequences of two-dimensional TEC maps over Japan provide a tool to identify LSTIDs.



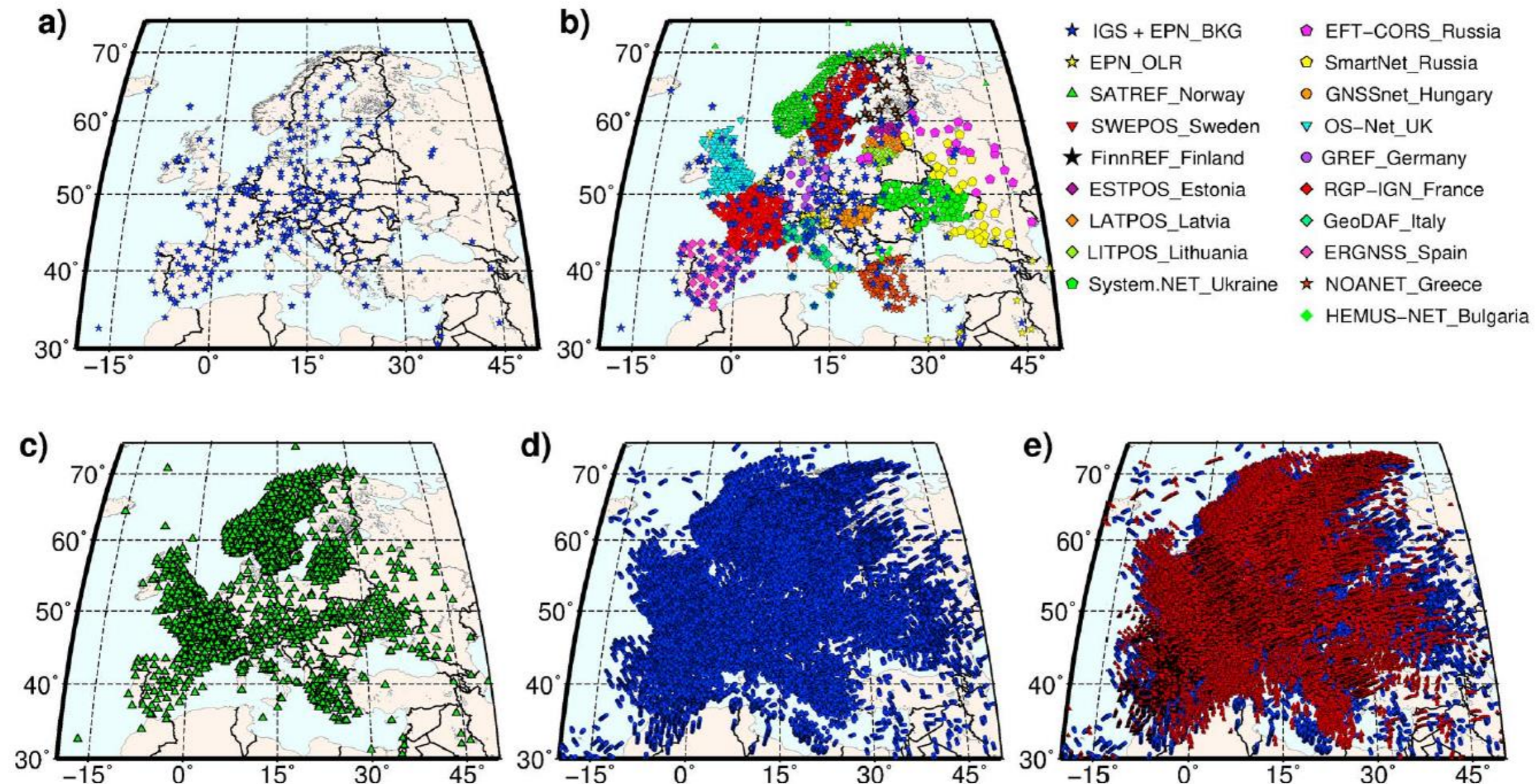
Borries et al. 2017

Study of the geomagnetic storm on 20 November 2003. Using TEC maps, IMAGE magnetometers and ionosonde data.

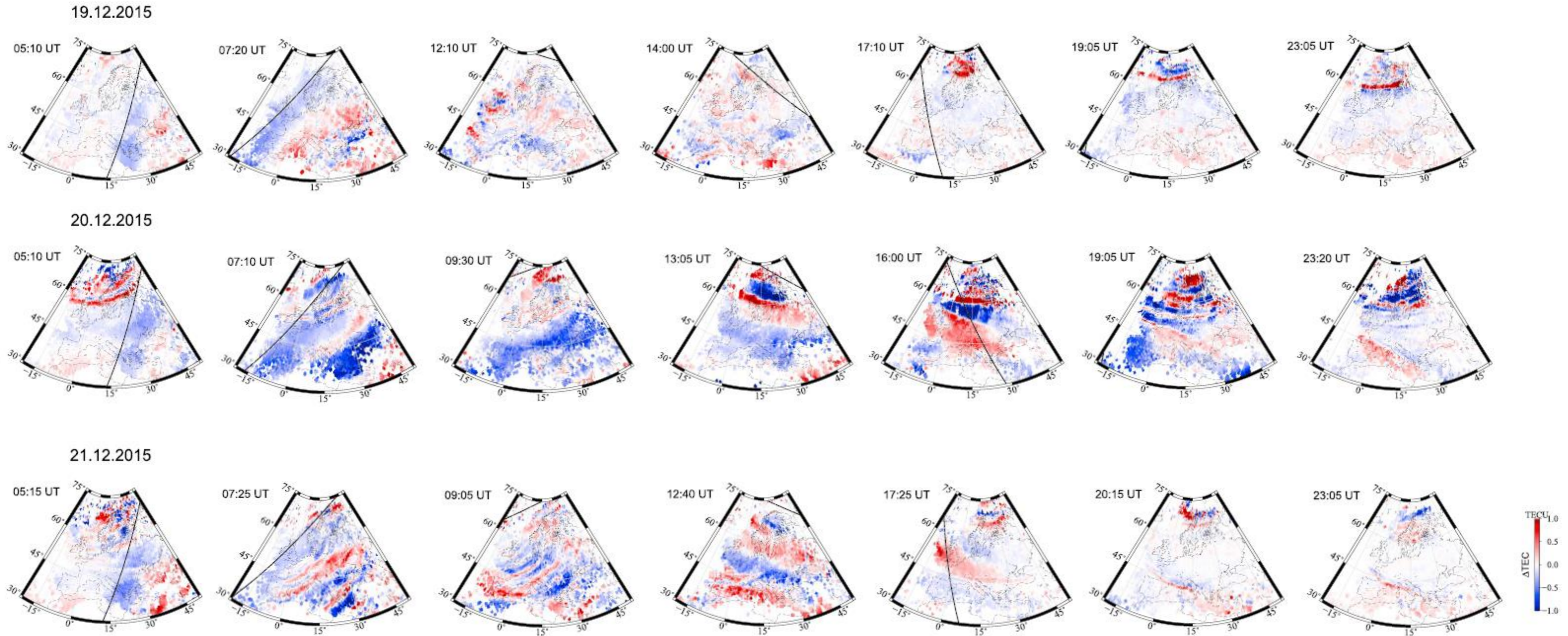


Cherniak and Zakharenkova 2018

Study of the origin, occurrence and propagation of LSTID over Europe during 19-21 December 2015 geomagnetic storm. Analysis of the TEC perturbation component supported by GPS and GLONASS.

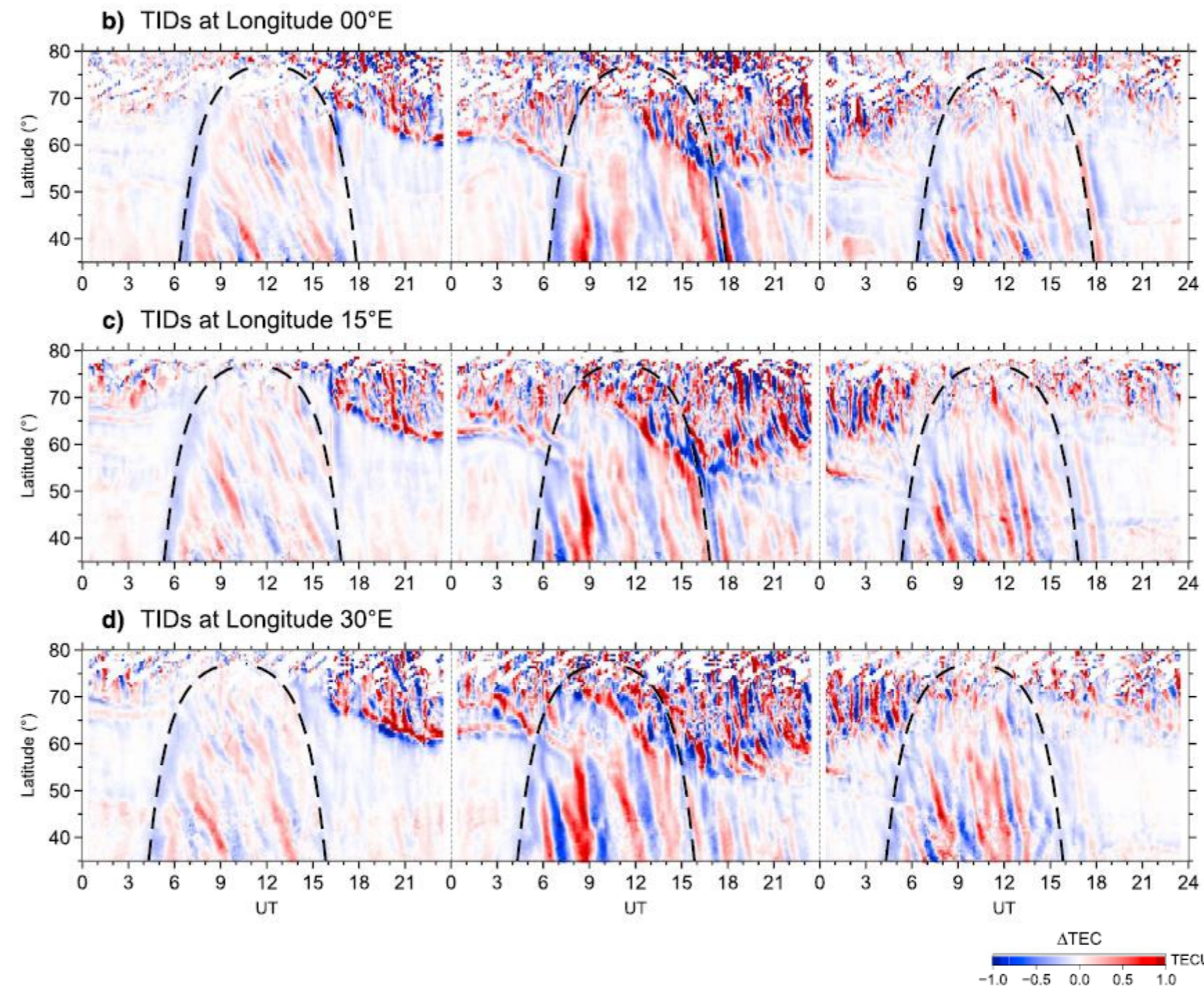


Cherniak and Zakharenkova 2018



Cherniak and Zakharenkova 2018

Keograms of TEC perturbations along three geographical longitudes (0, 15, and 30°E) during 19–21 December 2015. Black dashed line shows the solar terminator location





THANK YOU for ATENTION

- **Comments?**
- **Questions?**
- **Suggestions?**